Activation of novel secretoneurin circuits in ovulating zebrafish

Victoria Spadacini

Thesis submitted to the University of Ottawa
in partial Fulfillment of the requirements for the Master's degree in Biology

Department of Biology
Faculty of Science
University of Ottawa

Abstract

The hypothalamus-pituitary-gonad (HPG) axis is central to vertebrate reproduction. Hypothalamic neurons release the gonadotropin-releasing hormone (Gnrh) which stimulates the synthesis and release of the gonadotropins hormone (Lh) and follicle stimulating hormone (Fsh) in the anterior pituitary. Gonadotropins trigger and regulate essential reproductive events including spermatogenesis, gametogenesis, oocyte maturation, ovulation, and modulates sexual behaviours. Gnrh is considered the initiator of reproduction because it stimulates the Lh surge that in turn triggers ovulation. However, the novel neuropeptide secretoneurin (SN) can stimulate Lh release independent of Gnrh and mutations of the two SN precursor genes (*scg2a* and *scg2b*) result in significant reproductive deficits in zebrafish, most notably in ovulation and courtship behaviours. Thus far, there have been no demonstrations that SN-producing neurons are specifically activated prior to or during ovulation; this critical step is the focus of this thesis project. We tested the hypothesis that SNa is involved in the ovulatory process in female zebrafish because neurons are activated prior to ovulation. The main objective of this project was to determine when during the ovulatory cycle SNa neurons are being activated. We first validated a mouse anti-phospho-ERK1/2 primary antibody not yet tested in zebrafish and verified phospho-ERK as an effective biomarker for neuron activation through blocking immunoreaction with a phospho-peptide of the targeted ERK epitope and glutamatergic stimulation of key neuroendocrine regions. Using this antibody, activation of SNa neurons in the preoptic area (POA) was investigated as well as SNa action on Lh cells in the pituitary following SNa intraperitoneal injection. In the preoptic area, magnocellular neurons immunoreactive for SNa were progressively activated within the periovulatory window, with activation levels peaking at the time of presumptive ovulation (8:30h). At the time of the Lh surge (5:00h), 9.9% of SNa positive cells were active in the POA, increasing to 21% at ovulation. Intraperitoneal injection of a low (1 nmol/g) and high (2.5 nmol/g) dose of SNa in mature females isolated from males stimulated ovulation to a level equivalent to those injected with human chorionic gonadotropin (hCG). The low and high dose stimulated ovulation in 58% (7/12) and 75% (9/12) females respectively, compared to 83% (11/12) in the hCG group. Additionally, injections of both doses resulted in activation of Lh pituitary cells, with a 5.5-fold increase observed in ovulated fish injected with high dose SNa compared to unovulated saline injected controls. These results demonstrate that SNa neuronal networks are active prior to ovulation and

are likely modulating Lh cell activity in the pituitary. These data support the hypothesis that the Scg2/SN system plays a stimulatory role as a reproductive hormone in zebrafish.

Résumé

L'axe hypothalamus-hypophyse-gonade (HPG) joue un rôle central dans la reproduction des vertébrés. Les neurones hypothalamiques libèrent l'hormone de libération des gonadotrophines (Gnrh) qui stimule la synthèse et la libération de l'hormone gonadotrope (Lh) et de l'hormone folliculo-stimulante (Fsh) dans l'hypophyse antérieure. Les gonadotrophines déclenchent et régulent des événements reproductifs essentiels, notamment la spermatogenèse, la gamétogenèse, la maturation des ovocytes, l'ovulation, et modulent les comportements sexuels. La Gnrh est considérée comme l'initiateur de la reproduction car elle stimule la poussée de Lh qui, à son tour, déclenche l'ovulation. Cependant, le nouveau neuropeptide sécrétoneurine (SN) peut stimuler la libération de Lh indépendamment de la Gnrh et les mutations des deux gènes précurseurs de la SN (*scg2a* et *scg2b*) entraînent des déficits reproductifs significatifs chez le poisson zèbre, notamment en ce qui concerne l'ovulation et les comportements de parade nuptiale. Jusqu'à présent, il n'a pas été démontré que les neurones producteurs de SN sont spécifiquement activés avant ou pendant l'ovulation ; cette étape critique est au centre de ce projet de thèse. Nous avons testé l'hypothèse selon laquelle le SNa est impliqué dans le processus d'ovulation chez le poisson zèbre femelle parce que les neurones sont activés avant l'ovulation. L'objectif principal de ce projet était de déterminer à quel moment du cycle ovulatoire les neurones à SNa sont activés. Nous avons d'abord validé un anticorps primaire anti-phospho-ERK1/2 de souris qui n'avait pas encore été testé chez le poisson zèbre et nous avons vérifié que le phospho-ERK était un biomarqueur efficace pour l'activation des neurones en bloquant l'immunoréaction avec un phospho-peptide de l'épitope ERK ciblé et la stimulation glutamatergique de régions neuroendocrines clés. Cet anticorps a permis d'étudier l'activation des neurones SNa dans l'aire préoptique (POA) ainsi que l'action de la SNa sur les cellules Lh de l'hypophyse après injection intrapéritonéale de SNa. Dans l'aire préoptique, les neurones magnocellulaires immunoréactifs pour la SNa ont été progressivement activés au cours de la fenêtre périovulatoire, les niveaux d'activation atteignant leur maximum au moment de l'ovulation présumée (8h30). Au moment de la poussée de Lh (5:00h), 9,9% des cellules SNa positives étaient actives dans la POA, passant à 21% au moment de l'ovulation. L'injection intrapéritonéale d'une dose faible (1 nmol/g) et élevée (2,5 nmol/g) de SNa chez des femelles

matures isolées de mâles a stimulé l'ovulation à un niveau équivalent à celui des femelles ayant reçu une injection de gonadotrophine chorionique humaine (hCG). Les doses faible et élevée ont stimulé l'ovulation chez 58 % (7/12) et 75 % (9/12) des femelles respectivement, contre 83 % (11/12) dans le groupe hCG. En outre, les injections des deux doses ont entraîné l'activation des cellules hypophysaires Lh, avec une augmentation de 5,5 fois observée chez les poissons ovulés injectés avec la dose élevée de SNa par rapport aux contrôles non ovulés injectés avec de la solution saline. Ces résultats démontrent que les réseaux neuronaux SNa sont actifs avant l'ovulation et modulent probablement l'activité des cellules Lh dans l'hypophyse. Ces données soutiennent l'hypothèse selon laquelle le système Scg2/SN joue un rôle stimulant en tant qu'hormone de reproduction chez le poisson zèbre.

Acknowledgements

First and foremost, I want to extend the sincerest thank you to my supervisor Dr. Vance Trudeau. Finishing this thesis signifies the end of a challenging but extremely gratifying two and a half years, and I could not have done it without your constant support and guidance. Your encouragement throughout this project allowed me to build confidence as a scientist and has helped me to develop invaluable skills that will stay with me throughout my life beyond academia. The commitment you have to your students both inside and outside of the lab is remarkable, I am lucky to have you as a mentor. I would also like to thank my thesis committee, Dr. Michael Jonz and Dr. Tuan Bui for the support and help they have provided on this project through their valuable feedback and suggestions.

To my current lab mates and previous members of Teamendo, thank you so much for all the help you have provided throughout the entirety of my time in the lab, helping with experiments and giving me suggestions and support when I've felt stuck. It has been such a pleasure to work with and get to know everyone in the lab. Thank you to Dr. Chunyu Lu and Brianna Raven for your help in peptide synthesis. I would like to extend a special thank you to Dr. Peng Di, and Udeesha Erandani. Peng Di taught me the immunohistochemistry technique that has become the hallmark of my project, you will forever be the immuno-master! Udeesha, thank you for being the person I have looked to and been able to lean on in times of frustration and failure, and for the enthusiasm and encouragement you have shown me since day one. You are a brilliant scientist and friend. I would also like to thank Andrew Ochalski for helping me with all the microscopy work. I would like to acknowledge the University of Ottawa for its financial support throughout this Masters.

Finally, I would like to thank all my family and friends, old and new, who have continued to support and encourage me every step of the way, making moving away from home again a little less difficult. To the Weiss-Reids, I cannot thank you enough for taking me in these last few months, you are all so amazing. To my siblings, and most importantly my parents, I would not be here without your unwavering support, confidence, and love. You have believed in me even when I could not believe in myself, I love you all so much!

Table of Contents

List of Figures

Abbreviations and Terminology

AMPA	α-amino-3-hydroxy-5-methyl-4-isoxazole propionic acid
AH	Adenohypophysis
Avp	Arginine vasopressin
Avt	Arginine vasotocin
DA	Dopamine
dpf	Days post fertilization
ERK	Extracellular signal-regulated kinases
EtOH	Ethanol
Fsh	Follicle stimulating hormone
fshb	Follicle stimulating hormone beta
Gnih	Gonadotropin-inhibitory hormone
Gnrh	Gonadotropin releasing hormone
hCG	Human chorionic gonadotropin
hpf	Hours post fertilization
HPG	Hypothalamus-pituitary-gonad
Hyp	Hypothalamus
ICC	Immunocytochemistry
IF	Immunofluorescence
IHC	Immunohistochemistry
i.p	Intraperitoneal
ir	Immunoreactivity
Ist	Isotocin
Kp	Kisspeptin
Lh	Luteinizing hormone
lhb	Luteinizing hormone beta
MEK	Mitogen-activated protein kinase
mpf	Months post fertilization
n	Nano
NaCl	Sodium chloride; saline
NH	Neurohypophysis
NMDA	N-methyl-D-aspartate
OB	Olfactory bulb
Oxt	Oxytocin
pERK	Phosphorylated extracellular signal-regulated kinases
PC	Prohormone convertase
PI	Pars intermedia
Pit	Pituitary
PKC	Protein Kinase C
PM	Magnocellular preoptic nucleus

PMg	Gigantocellular part of the magnocellular preoptic nucleus
POA	Preoptic area
PPa	Anterior part of the parvocellular preoptic nucleus
PPD	Proximal pars distalis
PPp	Posterior part of the parvocellular preoptic nucleus
PN	Pars nervosa
PT	Pars tuberalis
RPD	Rostral pars distalis
RP3V	Rostral periventricular area of the third ventricle
Scg2	Secretogranin 2
SN	Secretoneurin
TALEN	Transcription activator-like effector nucleases
µ	Micro
WB	Western Blot
WT	Wildtype

Chapter 1. General Introduction

1.1 Rationale, hypothesis, and objectives

The hypothalamic-pituitary-gonadal (HPG) axis is the main endocrine axis controlling vertebrate reproduction. Governed by a variety of independent, and integrated neural networks, this axis serves to control hormone release from the pituitary, and in turn controls downstream reproductive events including spermatogenesis and gametogenesis, oocyte maturation, and ovulation. Historically and largely based on evidence from numerous mammalian models, gonadotropin-releasing hormone (Gnrh) has been considered indispensable to vertebrate reproduction. Viewed as the master controller and initiator of the HPG axis, hypothalamic Gnrh serves to initiate and stimulate anterior pituitary release of gonadotropins luteinizing hormone (Lh) and follicle stimulating hormone (Fsh), both of which act at the level of the gonads to regulate gonadal development, sex steroid production and successful release of eggs in females and sperm in males (Somoza et al., 2020; Trudeau, 2021). Teleosts, such as goldfish, medaka, and zebrafish, are commonly used models in neuroendocrine research, due to their brain-pituitary physiology. Unlike mammals who release hypophysiotropic hormones into the median eminence portal blood system to be distributed to the pituitary, teleosts have direct innervation of the pituitary by hypothalamic neurons (Trudeau & Somoza, 2020; Trudeau, 2021; Fontaine et al., 2022), making them exceptional targets to investigate and track specific neuropeptides and trophic hormone systems in different physiological contexts. Gene mutation and knockout studies of either one or both Gnrh paralogs in zebrafish and medaka have begun to reveal that Gnrh may not be the master controller of reproduction. Other hormones, neuropeptides and neurotransmitters may play important roles in controlling the reproductive axis.

One such hormone is secretoneurin (SN). It is a 31-34 amino acid neuropeptide derived from a larger precursor protein secretogranin-2 (Scg2) and has emerged as a candidate in teleost reproductive control. Teleosts have two Scg2/SN variants, Scg2a and Scg2b which produce the peptide products SNa and SNb, respectively. Neurons expressing Scg2a/SNa are in the olfactory bulb, clustered in the magnocellular preoptic nucleus, and hypothalamus; SNa cells are also located in the pituitary (Canosa et al., 2011; Mitchell, Zhang, et al., 2020). Recent and past work from our lab has revealed reproductive functions of SNa, with SNa successfully increasing gonadotropin subunit mRNA levels (Zhao et al., 2010). The generation of double *scg2a-/-*, *scg2b-/-* TALEN frameshift mutant zebrafish revealed significant reproductive deficits, including reduction of

neuropeptidergic and pituitary genes regulating reproduction such as *gnrh3, oxt, avp, lhb, fshb, cga* in females, and significantly reduced spawning to less than 10% (Mitchell et al., 2020). Gene expression of *oxt* and *gnrh3*, *lhb*, and *fshb* were reduced in both the *scg2a-/-* and *scg2b-/-* single mutants, with *gnrh3* levels being significantly lower in the *scg2a-/-* fish. Females scg2a-/- mutants specifically had a 90% decrease in *lhb* pituitary expression. Spawning success of the single mutants decreased from wildtype (WT) by 29% and 40% in the *scg2a-/-* and *scg2b-/-* fish, respectively. Mutation of *scg2a* resulted in significant impairment to ovulation in females (Mitchell et al., 2020), though injection of SNa can successfully stimulate ovulation in WT female zebrafish completely independent of male presence (Peng, 2022). Levels of SNa peptide in the whole brain and pituitary of wildtype females increase throughout the periovulatory period, peaking around the time of the presumptive Lh surge (Peng, 2022). Thus, the Scg2a/SNa system is proposed to play some role in regulating the teleost reproductive axis, likely promoting successful ovulation through effects on Lh. However, to date there have been no direct demonstrations that SNa producing neurons are activated prior to ovulation. Therefore, in this project, we used WT zebrafish to investigate the activity of SNa by tracking phospho-ERK — a neuronal activation biomarker — within the periovulatory period.

We tested the hypothesis that SNa is involved in the ovulatory process in female zebrafish because neurons are activated prior to ovulation. The main objective of this project is to determine when during the ovulatory cycle SNa neurons are being activated. The specific objectives of this research were to:

1. Validate a mouse anti-phospho-ERK1/2 primary antibody not yet tested in zebrafish and verify phospho-ERK as an effective biomarker for neuron activation (Chapter 2).
2. Investigate the activation of SNa neurons in the brain throughout the periovulatory period (Chapter 3).
3. Perform intraperitoneal injection of SNa to investigate the relationship between SNa and Lh in the pituitary (Chapter 4).

Below is a review of key aspects regarding the HPG-axis, neuroendocrine factors implicated in reproductive control, and ovulation. We then present data chapters summarizing the three main objectives. Each chapter is presented as an individual manuscript. Necessarily there is some level of redundancy in introductory material but each chapter addresses a distinct aspect of zebrafish

neuroendocrine physiology. For convenience, terminology used throughout will follow zebrafish nomenclature.

1.2 Hypothalamus-pituitary-gonadal (HPG) axis

The activity of the hypothalamus-pituitary-gonad (HPG) axis controls vertebrate reproduction (Kanda, 2019; Trudeau, 2021). Internal cues from an array of hormones and neuropeptides as well as external cues (i.e., temperature, photoperiod, and pheromones) dynamically regulate the reproductive system to promote reproductive success of both sexes (Espigares et al., 2017; Trudeau, 2021). The structure and cell types localized in the hypothalamus are highly conserved, allowing the hypothalamus to be separated into four main parts: preoptic, tuberal, anterior, and mammillary regions (Xie & Dorsky, 2017). The preoptic area (POA) is a major neuroendocrine control center, characterized by magnocellular and parvocellular neurosecretory cells (Wullimann et al., 1996). In mammalian species, hypophysiotropic neurons project to the median eminence where they are released and transported via the portal blood system to perfuse endocrine cells in the adenohypophysis (AH). In teleosts the median eminence was lost over evolutionary time and hypophysiotropic neurons project directly to the AH (Casteel & Singh, 2022). The pituitary is critical for hormonal regulation, acting as the bridge between the hypothalamus and peripheral organs and tissues. The adenohypophysis and neurohypophysis (NH) divide the teleost pituitary. The AH contains several endocrine cell type populations, divided in teleosts based on cell shape and size into the pars intermedia (PI), pars pars tuberalis (PT), and pars distalis which can be further divided into the rostral pars distalis (RPD, anterior) and the proximal pars distalis (PPD, medial) (Fontaine et al., 2022). The PPD houses gonadotrophs, which are directly linked to reproduction and the HPG axis by their release of gonadotrophs.

Spermatogenesis, gametogenesis, gonadal maturation, and gonadal secretion of sex steroids are all primarily regulated through the HPG axis through gonadotropin-releasing hormone (Gnrh) action (Kanda, 2019). Different vertebrate species express different Gnrh paralogs that have evolved over time, each of which have slightly different sequences and embryonic origins (Norris & Carr, 2021). Mammalian species can express Gnrh1 and Gnrh2, and teleost fish express two or three Gnrhs, with a significant number expressing Gnrh1, 2 and 3 (Trudeau, 2021; Zohar et al., 2021). Most teleosts, including the popular *Danio rerio* (zebrafish), express Gnrh2 and Gnrh3, with Gnrh3 neurons specifically being shown to play two specific hypophysiotropic and neuromodulatory roles in controlling pituitary and gonad functions (Y. Zhao et al., 2013). Cell

bodies of Gnrh neurons originate in the arcuate nucleus, and preoptic area, located within the hypothalamus in mammals (Casteel & Singh, 2022), but just outside the hypothalamic region and specifically in the preoptic area of the teleost telencephalon (Wullimann et al., 1996). Specifically, teleost Gnrh neurons, as well as other hypophysiotropic neurons, project into the pituitary and directly innervate or are in close proximity to their target cells (Trudeau, 2021; Trudeau & Somoza, 2020).

Gnrh neurons release the Gnrh peptide to act on gonadotroph cells in the anterior pituitary to stimulate the synthesis and secretion of the two gonadotrophs luteinizing hormone (Lh) and follicle stimulating hormone (Fsh) (Kanda, 2019; Trudeau et al., 2023). Fsh and Lh are glycoprotein hormones containing one common alpha chain, and a variable beta chain that give them their specificity (Kumar, 2005; Trudeau, 2021). These two hormones signal through binding G-protein coupled receptors that activate downstream signalling cascades through the PKC/MEK/ERK1/2 and AKT pathways (Casarini et al., 2018). The gonadotropins activate both male and female gonadal cells and are directly responsible for stimulating gonadal development, sperm production, follicle maturation, ovulation, and the production of key sex steroids such as androgens and estrogens (Trudeau, 2021). Gonadotropin involvement promoting proper reproduction and modulation of the HPG axis through negative feedback is evident through a variety of knockout and targeted mutation studies. Disruptions with the proper production or functioning of Lh, Fsh, or both result in inability to ovulate, delayed or disrupted gonadal development (Z. Zhang et al., 2015), disrupted gamete production, and infertility (Ma et al., 2004; Kumar, 2005; Zhang et al., 2015).

Gnrh has been considered the master initiator of reproduction, especially important in promoting the Lh surge required to trigger ovulation in both mammalian and teleost fish species (Goodman et al., 2022; Kanda, 2019; Ma et al., 2004; Trudeau, 2021). Laser ablation of Gnrh3 neurons in zebrafish resulted in arrested oocyte development, with partial ablation resulting in abnormal oocyte development and significantly reduced fecundity (Abraham et al., 2010). TALENs-mediated Gnrh1 knockout in medaka significantly reduced levels of whole pituitary *lhb* mRNA, with both Gnrh1 and Lh knockout fish displaying significant deficiencies in ovulation (Takahashi et al., 2016). However, striking evidence from this and several other Gnrh knockout studies directly contradict what has thus far been considered dogma in vertebrate reproduction. Though deficiencies to ovulation were observed in the Gnrh and Lh knockout medaka, Takahashi's

group found that males remained fertile (Takahashi et al., 2016). Additionally, upon targeting Gnrh3 in zebrafish with TALEN-mediated mutagenesis, another group surprisingly found that impacts on gonadotropin subunit mRNA levels observed in developing larvae returned to normal in adults, and there was no significant impact on reproduction overall (Spicer et al., 2016). Double knockout zebrafish for both Gnrh2 and Gnrh3 yielded the same results, as *fshb*, *lhb* and *cga* (the common alpha subunit) expression all showed no significant change in adult fish (Marvel et al., 2018). These findings suggest the existence of an as yet, ill-defined, compensatory mechanism that may rescue reproductive function from disruptions in portions of the vertebrate reproductive axis previously considered indispensable. Such potential compensatory mechanisms could involve regulators of Gnrh neurons, such as kisspeptins (Kp) (De Tassigny et al., 2008; Harter et al., 2018; Y. Zhao et al., 2014) and gonadotropin-inhibitory hormone (Gnih) (Ducret et al., 2009), or perhaps from other neuropeptides like secretoneurin (SN) (Mitchell, Mikwar, et al., 2020; Trudeau, 2021).

1.3 Neurochemical regulation of teleost reproductive axis

1.3.1 Secretoneurin

Secretoneurin (SN) is a neuropeptide recently implicated in the regulation of vertebrate reproduction. Secretoneurin is a short 31-34 amino acid long peptide highly conserved from lampreys to humans, originating from the larger 588-624 amino acid long precursor secretogranin-II (Scg2) (Canosa et al., 2011; Trudeau et al., 2012; Vaudry & Conlon, 1991). Like processing of another well studied anterior pituitary hormone ACTH, derived from POMC precursor (Schnaber et al., 1989), Scg2 is proteolytically processed within neuronal and some endocrine cell secretory vesicles by prohormone convertases into a series of smaller peptide fragments, the most conserved of them being SN (Canosa et al., 2011; Vaudry & Conlon, 1991). Prohormone convertase 1 (PC1) and 2 (PC2) can both cleave Scg2 at dibasic sites to generate a variety of peptide fragments of intermediate length, though in neurons specifically, it is only through processing by PC1 that SN is produced (Hoflehner et al., 1995). Secretoneurin was among the first group of peptides identified by proteolytic processing of the granin family (Kirchmair et al., 1993), with its functions being the least understood until recently (Troger et al., 2017). Interestingly, Scg2 is processed to SN the most in the brain, with levels reaching 89-97% in comparison to only 49% or 26% in the adrenal medulla and anterior pituitary of the rat, respectively (Kirchmair et al., 1993; Trudeau et al., 2012). This highlights the primary role of SN as a neuropeptide. Smaller SN fragments such as (SNa_{1-14}

and SNb_{1-19}) have been identified from the zebrafish model in our lab (Lu, Peng and Trudeau, unpublished data), their bioactivities and potential functions remain unknown.

Secretoneurin contains a core sequence of YTPQ-X-L-X_8-EL across all vertebrates in which it has been found (Mitchell, Mikwar, et al., 2020; E. Zhao et al., 2009). Between mammalian species, the Scg2 gene is around 79 to 87% identical, with mammals, birds, and amphibians and other tetrapods expressing only one version and producing one SN paralog (Mitchell, Mikwar, et al., 2020). Likely due to their whole genome duplication event, a different situation exists in teleost fish. Teleosts express two distinct paralogs of Scg2 (Scg2a and Sgc2b), each of which produce a distinct form of SN, designated SNa and SNb respectively (Trudeau, 2021). Although not definitive, SNa in teleosts is likely the form of the gene that has been conserved in all vertebrates, while SNb is teleost specific (Trudeau et al., 2012).

Several groups have demonstrated that SN is regulated by Gnrh to promote Lh secretion from gonadotrophs in vertebrate species. Work in goldfish have revealed that Gnrh agonist treatments stimulated *lhb* expression as well as *scg2* expression, and that the sex steroid testosterone regulates *scg2* and *lhb* levels in a negative feedback fashion (Samia et al., 2004). Other *in vivo* treatments of isolated rat pituitary cells (Wei et al., 1995) and the mouse LβT2 gonadotroph cell line (Nicol et al., 2004) showed significant increase in both *lhb* and *scg2* pituitary expression after treatment with Gnrh, indicating that Scg2/SN in the pituitary is stimulated by Gnrh (Fig 1.1). When treated with a dopamine receptor blocker, domperidone, SNa stimulates Lh release from goldfish pituitary fragments more than 2-fold (E. Zhao, Basak, & Trudeau, 2006). Furthermore, treatment with goldfish and mouse SNa directly stimulates Lh secretion from dispersed goldfish pituitary cells (Zhao et al., 2006) and mouse LβT2 cells (Zhao et al., 2011) respectively, independent of a Gnrh agonist. This strengthens the hypothesis that SN is important for stimulating gonadotropin release.

It is hypothesized that SN can exert a regulatory role on the synthesis and release of Gnrh and Lh. For example, TALENs-mediated frameshift mutations of both forms of Scg2 resulted in significant reductions in *gnrh3* expression in the telencephalon and hypothalamus of both sexes, as well as significantly decreased pituitary expression of all gonadotropin subunits (*lhb, fshb,* and *cga*). Female scg2a-/- single mutants showed a 90% reduction in *lhb* expression compared to WT (Mitchell et al., 2020). Conversely, SNa intraperitoneal (i.p) injection increased hypothalamic *gnrh3* expression and increased pituitary lhb expression 7.7-fold from saline injected controls.

(Mitchell et al., 2020; Peng D, 2022). However, the mechanism by which it may be regulating the activity of Gnrh and Lh remains unknown (Zhao et al., 2011). To date, a receptor for SN has not been identified, though numerous groups including our lab have tried with no success. Some evidence suggests that SN targets a G-protein coupled receptor present on gonadotrophs acting via cyclic-AMP and MAPK/MEK signalling pathways (Zhao et al., 2011) and likely an AKT-dependent pathway (B. Tao et al., 2018). AKT signalling is not unique to GPCRs and can be enhanced by factors that do not act through GPCR signalling, therefore SN signalling through a GPCR remains speculative.

Secretoneurin-immunoreactivity is localized mainly in the hypothalamus and pituitary of various vertebrate species. In the goldfish model, SN immunoreactivity was observed in the olfactory bulb, preoptic nucleus, the lateral part of the lateral tuberal nucleus and posterior periventricular nucleus of the hypothalamus, with SN fibers projecting into dorsal part of the dorsal telencephalon, ventral and lateral parts of the ventral telencephalon, and the periventricular preoptic nucleus, in addition to the pituitary itself (Canosa et al., 2011). In situ hybridization in zebrafish corroborated these findings and revealed *scg2a* and *scg2b* expression in the central, dorsal, ventral, and lateral nucleus of the ventral telencephalon, strong expression in caudal, dorsal, and ventral periventricular hypothalamic nuclei, and throughout the pituitary but predominantly the neurointermediate lobe (Mitchell, 2018). Furthermore, the most discernible SN immunoreactivity is located within magnocellular and parvocellular cells in the preoptic nucleus, and within prolactin (PRL) cells of the rostral pars distalis (RPD) of the goldfish, and some other identified cells in the zebrafish (Peng, 2022). Strong immunoreactivity of SN has been observed co-localized within preoptic Ist-positive neurons that terminate in the neurointermediate lobe of the goldfish (Canosa et al., 2011; Zhao et al., 2009) and zebrafish (Peng 2022) pituitary, suggesting the potential co-release of SN and Ist during teleost reproduction in addition to independent SN release from the hypothalamus and pituitary (Fig 1.1).

With respect to sexual behaviour and successful spawning, our lab has provided strong evidence with the first Scg2 mutant model that Scg2/SN has a pivotal role in controlling reproduction. TALENs-mediated frameshift mutations in both zebrafish paralogs (Scg2a and Scg2b) generated by our lab resulted in severely impaired mating behaviour and a significant reduction in ovulation (Mitchell et al., 2020). Compared to 11 of 15 wildtype females, only 1 of 10 double mutants successfully ovulated, despite the observed normal oocyte maturation, gonadal

development, and ovarian function in the mutants. Notably, spawning success in the double mutants was rescued and not significantly different than wildtypes upon injection with either SNa or SNb (Mitchell 2018; Mitchell et al., 2020b), reinforcing the role of SN as a reproductive hormone.

1.3.2 Nonapeptides

Nonapeptides are an ancient, highly conserved family of neuropeptides that arose from as a result of the vasotocin gene duplication (Acher & Chauvet, 1995). The very conserved structure characterizing these cyclic peptides include two half cysteine residues at position 1 and 6 forming a disulfide bridge, and an glycine amide at position 9. Position 8 categorizes members into either basic or neutral nonapeptide families (Urano & Ando, 2011). Oxytocin (Oxt) and arginine vasopressin (Avp) (also known as fish Isotocin, Ist, and arginine vasotocin, Avt) are the two most well-known members of the family, synthesized in preoptic magnocellular neurons which project into the posterior pituitary (Canosa et al., 2011; Goodson, 2008; Goodson et al., 2012). Gnrh can modulate Oxt and Avp release, highlighting a link of nonapeptides to the HPG axis. In rainbow trout, Gnrh fibers have been detected in proximity of vasotocin neurons, and administration of Gnrh increases cell-type specific calcium pulses in these neurons (Saito 2003). Additionally, vasopressin release is stimulated successfully with a highly selective GnRH agonist in rats (Boczek-Leszczyk et al., 2010). Histrelin, another highly selective Gnrh agonist, stimulates secretion of oxytocin in the rat hypothalamo-neurohypophysial system (Juszczak & Boczek-Leszczyk, 2010). Moreover, Oxt is important in the release of Lh (Trudeau, 1997), as injection of Oxt in sexually regressed increased Lh release by over 150% relative to controls (Popesku et al., 2011). This highlights oxytocinergic and vasopressinergic neurons as likely circuits modulating and interacting with the HPG axis.

Oxt/Ist and Avp/Avt are important for social-sexual behaviour (Goodson & Bass, 2001; Mennigen et al., 2022a). In mammals, Oxt is also associated with ovulation and stimulation of the Lh surge (Johnston et al., 1990; Melli et al., 2007) but little is known about the mechanisms involved, like SNa. In the goldfish model, similar to various mammalian species, magnocellular Ist neurons that produce SNa exhibit robust projections to the posterior pituitary (Zhao et al., 2009; Canosa et al., 2011). Neurons identified by SNa-immunoreactivity, expressing either SNa alone or both Ist and SNa terminate in proximity to gonadotrophs in the PPD (Canosa et al., 2011, Peng, 2022). In the weakly electric fish *Brachyhypopomus gauderio*, SN coexists with Ist and Avt in

both cells and fibers of the POA (Pouso et al., 2015). Considering the significance of Oxt (Mennigen et al., 2022) and suggested involvement of SNa in reproductive behavior, and ovulation, it is crucial to investigate the interaction of nonapeptide and secretograninergic systems.

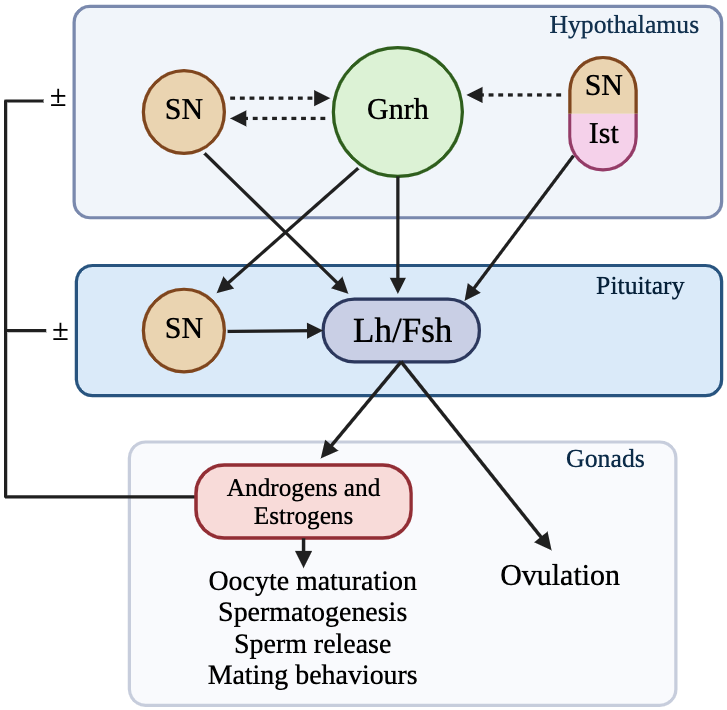

Fig 1.1 Simplified and generalized proposed model of neuroendocrine control of reproduction in teleosts. Solid arrows represent stimulation whereas dotted arrows represent a hypothesized but understudied relationship. Lines with ± represent positive or negative feedback regulation. SN, secretoneurin; Ist, isotocin; Gnrh, gonadotropin-releasing hormone; Lh, luteinizing hormone; Fsh, follicle stimulating hormone.

1.4 Teleost ovulation

Surge release of Lh the anterior pituitary triggers oocyte maturation and subsequent follicle rupture and oocyte release (Goetz & Garczynski, 1997; Tsafriri & Reich, 1999). Release of the mature oocyte from the follicle is the hallmark of ovulation, controlled by a variety of factors such as prostaglandins and serine proteases (Espey, 1980). These factors are also involved in inflammatory responses; thus, ovulation has been hypothesized as an inflammatory response-like process, characterized by dilation of ovarian vasculature, increase in circulation, and recruitment of leukocytes and thrombocytes to follicles just prior to ovulation upon Lh stimulation (Espey, 1980). Prior to ovulation, fish oocytes undergo dramatic changes in structure and composition,

requiring the separation of the oocyte from the granulosa layer via proteolytic cleavage and remodelling by proteases (Goetz, 1983; Goetz & Garczynski, 1997). Fish oocytes must complete germinal vesicle breakdown (GVBD) wherein following enlargement of the follicle, the oocyte migrates to the follicle periphery, mediated by various hormonal and steroidal inputs (Goetz, 1983).

Teleost final oocyte maturation is mediated by the production of steroids and steroid derivatives in the gonads in response to Lh, such as 17α,20β-dihydroxy-4-pregnen-3-one (DHP), also known as maturation-inducing hormone (MIH) (Nagahama & Yamashita, 2008). Though similarities certainly exist, teleost ovulation does differ from mammalian ovulation (Espigares et al., 2017). An important regulator of ovulation in vertebrates is photoperiod. However, since fish are induced ovulators, unlike mammals who are spontaneous ovulators, researchers can therefore manipulate the naturally occurring ovulatory cycle to induce ovulation and spawning when desired. The female counterpart of many fish species exhibits serial spawning in which they complete a full ovulatory cycle within 24 to 96 hours (Migaud et al., 2010). In zebrafish, this cycle is 24 hours long, and thus in research facilities they are often reared under the regimen of 10 hours of dark, 14 hours of light. Pheromones also play a role in stimulating ovulation and successful breeding. In both male and female teleosts, the timed release of pheromones following the Lh surge signals the other to prepare for spawning such as by inducing ovulation (Amagai et al., 2022), inducing the production of sex steroids in females such as 17,20β-DHP, and stimulating increase in male Lh to subsequently increase their milt production (fish seminal fluid) (Stacey & Pandey, 1975). By placing females and males together in the same tank with physical separation allows researchers to manipulate and induce ovulation to breed fish and study reproduction on a deeper level.

In addition to the role SN has been demonstrated to play in sexual behaviour, and the deficits observed in ovulation upon Scg2/SN mutants, our lab has recently uncovered that SN and Gnrh3 levels increase together at the time of the Lh surge, and that injection of SNa can successfully stimulate ovulation in mature female zebrafish in the absence of a male (Peng, 2022). Despite the published and unpublished data from our lab, there has been no direct demonstrations that the SN-producing neurons are activated prior to ovulation to date. This critical step will be the focus of my research, as well as investigating potential pituitary cell activation by SNa injections to explore the link between SNa and Lh within the reproductive axis.

1.5 Ethics statement

All experiments were approved by the University of Ottawa's Animal Care Protocol Review Committee and comply with the guidelines established and approved by the Canadian Council on Animal Care for the use of animals in research.

Chapter 2. Validation of mouse anti-p-ERK primary antibody to use in visualizing HPG signalling

2.1 Introduction

The field of neurobiology and studying the activity of at a cellular level in the brain are essential components of understanding the overall nature and role of hormones, neuropeptides, and neurotransmitters within vertebrate endocrine systems. A vast majority of the currently known factors responsible for controlling reproduction are produced and released from neurons or secretory cells residing in the brain. The olfactory bulbs (OB), pre-optic area (POA), hypothalamic nuclei, and pituitary are known locations for hormone and neuropeptide synthesis and release. Vertebrate olfactory bulbs contain primarily mitral cells, among others (Fuller et al., 2006). In teleosts, specifically zebrafish, these mitral cells are glutamatergic which serve primarily to process odor information (Edwards & Michel, 2002; Fuller et al., 2006; Kermen et al., 2013). Olfaction and odor processing are known to influence the feeding and reproductive behaviours in fish (Stacey & Kyle, 1983), implicating the OB as an area of reproductive control. The vertebrate POA is a main center involved in the social behaviour network (SBN) – aggression, communication, appetitive and consummatory sexual behaviour, social recognition, response to social stress, bonding, and parental care (Goodson, 2005) – governed strongly by arginine vasopressin-oxytocin family nonapeptides (Markham et al., 2019; Mennigen et al., 2022). In teleosts, the POA has been found to have large populations of arginine vasotocin (Avt) positive neurons (Foran & Bass, 1998; Almeida & Oliveira, 2015; Markham et al., 2019; Scaia et al., 2022b). In goldfish (Canosa et al., 2011) and zebrafish (Peng, 2022), SNa is found in POA neurons. Avt in the POA is modulated by Gnrh in rainbow trout (Balment et al., 2006), further highlighting the importance of the POA as a center for reproductive control. The teleost pituitary is the location of at least 6 main endocrine cell types responsible for modulating numerous different endocrine axes (Fontaine et al., 2022), existing as the middle location for control between the higher brain nuclei and downstream endocrine organs (i.e gonads, adrenals, pancreas, etc). Specific to reproduction, the pituitary is the main location of gonadotropin production and release (Lh and Fsh), both of which are essential to overall reproductive success in not only teleosts, but vertebrates in general. Thus, it becomes imperative to investigate the activation of different neural and secretory cells throughout the brain to fully characterize how, where, and most importantly when, these different HPG players exert neuroendocrine control over reproductive events.

Proteins such as phospho-S6 ribosomal protein (pS6) (Scaia et al., 2022b), pERK (Randlett et al., 2015) and Fos (Bakker et al., 2002; Taziaux & Bakker, 2015; Markham et al., 2019) are useful and robust biomarkers for measuring neuronal activation. Fos is the protein product of *c-fos*, an intermediate early gene and a transcription factor that is activated in neurons during firing (Taziaux & Bakker, 2015). Though a good indicator of neuronal activity used in studies focused on memory, mating, and sleep, among others, it has been documented to have poor temporal resolution and lower sensitivity (Baraban et al., 2005), as well as a very slow action time course and mRNA and protein responses in teleost fish (Baraban et al., 2005; Okuyama et al., 2011). Since the goal of this project is to measure neuronal activation at very specific time points throughout the zebrafish ovulatory period, a slower acting biomarker is not ideal.

Extracellular signal-related kinase (ERK) is a member of the MAP kinase signalling pathway. that becomes activated through phosphorylation upon stimulation via calcium influx into neuronal cells (Xia et al., 1996; Hussain et al., 2013). ERK is maintained in the cytoplasm, tethered by anchoring and scaffold proteins until it is activated (Chuderland & Seger, 2005). Activation occurs following the phosphorylation of the Thr and Tyr residues in its activation loop by MEK1/2. This triggers shuttling and translocation of ERK into the nucleus (around 50-70% of total ERK molecules (Chen et al., 1992), where it acts as a transcription factor, primarily regulating gene transcription of immediate early genes (IEGs), as well as others. It has also been found to regulate nuclear receptors, such as the estrogen receptor (ER) (Kato et al., 1995). Secondarily, some phosphorylated ERK (pERK) is held in the cytoplasm and translocated to cytoplasmic targets such as the mitochondria or Golgi apparatus (Wortzel & Seger, 2011).

MAPK/ERK pathway is involved in a host of cellular processes including proliferation, differentiation, motility, and survival, and is activated by different factors and molecules such as cytokines, growth factors, and neurotransmitters, among others. In neuronal systems, glutamate — a potent stimulatory neurotransmitter for teleosts — activates AMPA and NMDA receptors to trigger the MAPK/ERK cascade (Wang et al., 2007; Iwase et al., 2014). Thus, pERK can and has been used as a robust biomarker for neuronal activation (Randlett et al., 2015; Altmieme et al., 2019), documented to generate strong signals within 2 to 5 minutes of neuron stimulation in zebrafish (Hussain et al., 2013; Randlett et al., 2015) and rat (Ru-Rong Ji et al., 1999; Dai et al., 2002) models. As a transcription factor, it is mainly localized to the nucleus in its active form (Wortzel & Seger, 2011; Maik-Rachline et al., 2019), however it can be found and visualized in

the cytosol through paraffin immunohistochemistry (Brechbuhl et al., 2020). Here we validated a commercial primary pERK antibody not yet tested in zebrafish brain tissue through immunohistochemistry as means to verify its effectiveness as a robust biomarker. We did so through first visualizing baseline staining, followed by blocking pERK immunoreactivity by pre-absorption with a custom phosphorylated peptide. Finally, taking advantage of the stimulatory action of glutamate in vertebrate nervous systems, a positive control experiment was performed wherein the glutamate agonist S-AMPA was used to activate neurons in the adult female brain, to evaluate if there was a sufficient increase in pERK immunoreactivity following this stimulation, and thus pERK is a good biomarker for assessing neuron activation.

2.2 Materials and methods

2.*2.1 Experimental animal husbandry*

Experimental wildtype zebrafish were kept and bred in the University of Ottawa aquatics room. Fish were maintained in the rooms at 28˚C under a consistent photoperiod of lights-on from 0900h to 2300h. Wildtype zebrafish were provided by the Aquatics Facility at the University of Ottawa and were maintained and fed twice daily by Animal Care and Veterinary Staff. All experiments using zebrafish followed animal use protocols generated under the guidelines of the Canadian Council on Animal Care and were approved by the University of Ottawa's Animal Care Protocol Review Committee.

2.2.2 S-AMPA dosage and intraperitoneal injection

Stock solution of dissolved S-AMPA (5 µg/µl) was diluted further to identify a maximum dosage that does not induce any seizures following intraperitoneal injection. Tested dosages were 5.0 µg/g bodyweight, 3 µg/g bodyweight, 2.5 µg/g bodyweight, 2.0 µg/g bodyweight, 1.5 µg/g bodyweight, 1.25 µg/g bodyweight, and 0.625 µg/g bodyweight, with 0.6% NaCl (saline) as a control. Dosages were chosen based on previous work by Trudeau et al., 2011. Two to three males and females per dosage were anesthetized using 4.2% tricane methanesulfonate solution, injected with 10 µl/g of bodyweight S-AMPA using a 32-gauge Hamilton syringe, returned to their tanks, and allowed to recover for a minimum of 10 minutes. During this time, seizure activity was monitored. The maximum effective dosage not producing any seizure activity was 2.0 µg/g bodyweight and was used for all subsequent S-AMPA injections.

Intraperitoneal injections of saline or S-AMPA were performed on female zebrafish to stimulate neuron activation and verify phospho-ERK as a valid neuronal activation biomarker. All fish used were sexually mature and between 6-10 months post-fertilization (mpf). To synchronize their reproductive cycles, females were separated from males a minimum of two weeks prior to the injection experiment. On the day of injection, females were randomly assigned to one of three housing tanks, and then using a random number generator were assigned to either Saline 3 MIN (n = 7) or S-AMPA 3 MIN (n = 7) experimental groups. Females were anesthetized with 4.2% tricane methanesulfonate solution before being injected intraperitoneally with either 0.6% NaCl (pH=7; 10 µl/g body weight) or 2.0 µg/ul S-AMPA (10ul/g body weight) using a 32-gauge Hamilton syringe. Injections were performed between 10:00h and 12:00h. Fish were returned to individual static tanks to recover, and then were sacrificed on ice for dissection and fixation after 3 minutes.

2.2.3 Design and use of custom phospho-ERK peptide

Invitrogen, the producer of the pERK antibody does not provide a suitable blocking peptide that corresponds to the mouse anti-phospho-ERK1/2 monoclonal primary antibody (Cat# 14-9109-82) and the epitope it targets, so we designed a custom phospho-peptide identical to the epitope, including the two phosphorylated sites specific to this antibody. The amino acid sequence of the peptide is HTGFL(pT)E(pY)VATRW, this is a conserved sequence containing 2 phosphorylation sites in the vertebrate ERK protein (Appendix 1). The peptide was manufactured for us by AbClonal Technology with a purity of 98.025%. The phospho-peptide was diluted in ddH_2O to form a stock (0.5 mg/ml). The phospho-ERK primary antibody was then pre-incubated with either 5 µM, 10 µM, or 15 µM of this peptide for 24 hours at 4˚C, before treating the sections for immunofluorescence.

2.2.4 Brain dissection and paraffin embedding

Fish were sacrificed using a cold shock in an ice bath. Fish were taken, the skull flap was removed to allow for better penetration of the brain tissue during tissue processing, and placed in 4% paraformaldehyde for 24 hours for fixation. Samples were then washed with PBS three times for 20 minutes each and decalcified at room temperature using 0.5M EDTA for 6 days. Once decalcified, samples were again washed with PBS two times for 15 minutes and then dehydrated in an ethanol (EtOH) series of increasing concentrations (30%, 50%, 70%, 80%, and 99% EtOH

for 30 min, 30 min, overnight, 40 min, and 1 hour respectively). Samples were treated with 1:1 xylene and ethanol solution for 30 min, then two treatments with 100% xylene for 30 and 45 min. Finally, samples underwent a series of incubations in melted paraffin at 60˚C and then left to incubate in paraffin overnight.

All samples were embedded in paraffin blocks using metal molds the next morning. Heads were embedded in sagittal orientation. Once the paraffin cooled and set, the solidified blocks were removed from molds and stored at room temperature until sectioned. For sectioning, the Leica RM2255 Microtome was used to slice 8µm thick sagittal sections of brain tissue. Sections were mounted on glass microscope slides (Fisherbrand, cat#22-037-246). Slides were stored for a maximum of one week at room temperature in a sealed slide box before immunofluorescence.

2.2.5 Immunofluorescence

On the day of immunofluorescence treatment, all chosen slides were heated on a slide warmer at 60˚C for 30 min and then deparaffinized using xylene twice for 20 min. Slides were then rehydrated using an ethanol (EtOH) series of decreasing ethanol concentrations for 10 min each (99% and 95% EtOH twice, 70% once), and finally in PBS for 10 min.

For antigen retrieval, slides were incubated with an antigen retrieval buffer of 0.01M Sodium Citrate (pH 6.0) in an 84-90˚C water bath for 30 min. Slides were then removed, allowed to cool, washed with PBS 2 times for 2 min before being treated in a blocking buffer (1% skim milk, 0.3% Triton-100) at room temperature for 30 min. For immunofluorescence, all slides were first incubated overnight at 4˚C in primary antibodies, followed by secondary antibodies the next day:

1) Slides used to establish baseline pERK staining in female zebrafish brain and pituitary were incubated with mouse-anti-phosphoERK1/2 (Thr202, Tyr204) monoclonal antibody diluted in 1:100, 1:200, or 1:400 (Invitrogen, Cat# 14-9109-82). The next day after being washed again with 1xPBS, all slides were treated in the dark with Goat anti-Mouse IgG1 Cross-Adsorbed Secondary Antibody, Alexa Fluor™ 594 (Invitrogen, Cat# A-21125), diluted in 1:500.
2) Slides used to confirm specificity of primary antibody by blocking immunoreaction with custom designed phospho-ERK peptide were treated with one of three solutions: (a) regular primary antibody diluted 1:200 in blocking buffer, (b) blocking buffer alone with no primary antibody added (to test for any secondary antibody off target binding),

or (c) pre-absorbed primary antibody diluted 1:200 in blocking buffer (5uM, 10uM, or 15uM pERK epitope peptide). The next day after being washed again with 1xPBS, all slides were treated in the dark with Goat anti-Mouse IgG1 Cross-Adsorbed Secondary Antibody, Alexa Fluor™ 594 (Invitrogen, Cat# A-21125) at a 1:500 dilution.

3) Samples of fish injected with Saline or S-AMPA were treated with rabbit-anti-goldfish SN antiserum diluted 1:800, and mouse-anti-phosphoERK1/2 (Thr202, Tyr204) monoclonal antibody diluted 1:200 (Invitrogen, Cat# 14-9109-82). The next day after being washed again with 1xPBS, all slides were treated in the dark with Goat anti-Rabbit IgG (H+L) Cross-Adsorbed Secondary Antibody, Alexa Fluor™ 488 (Invitrogen, Cat# A-11008) and Goat anti-Mouse IgG1 Cross-Adsorbed Secondary Antibody, Alexa Fluor™ 594 (Invitrogen, Cat# A-21125), both diluted 1:500.

The rabbit-anti-goldfish SNa antiserum used was previously developed, tested, and validated by our lab through western blotting (WB), showing it recognizes any processed fragments containing the SNa epitope, including the Scg2a precursor peptide (E. Zhao, Basak, Crump, et al., 2006).

All slides were washed 2X with 1xPBS completely shielded from light. Slides were treated with 55 µl of SlowFade™ Diamond Antifade Mountant with DAPI (Invitrogen, cat# S36973) and mounted with 22x60 mm No. 1.5 coverslips (VWR, cat# 48393-221).

2.2.6 Cell counting and data collection

Samples were imaged using Zeiss Axio Imager.Z2 Upright Fluorescence Microscope with ApoTome.2. Serial images were taken of every other section on the slide, starting from the first section present. Different brain regions were identified through landmarks (Wullimann et al., 1996) and images were taken from identical sites. All images were collected as Z-stacks, and then processed using the Extended Depth of Focus function in ZEN 3.2.0. The brightness, contrast, and colour balance of each captured image were adjusted using FIJI in ImageJ.

For cell counting, a systematic random sampling strategy was applied, used by Canosa et al., 2011 and was adapted from Geuna, 2000. A 100 µm grid was applied to each image, and a set sample area was established for each different brain region (hypothalamus, pituitary, POA). Positive pERK-immunoreactive cells (cell profiles) were counted in each 100 µm x 100 µm box. The total number of cell profiles was added up for each section, and the average number of cell profiles was established by dividing the sum of all cell profiles of a particular brain region by the

number of sections analyzed for that fish. Images were coded and randomized by an independent party to minimize bias in counting.

2.2.7. Statistical analysis

Statistical analysis was performed using GraphPad Prism 9 Software (GraphPad Prism Inc.). The data was determined to be normally distributed via the Shapiro-Wilk normality test. Unpaired t-tests with Welsh's correction were then conducted to determine statistical significance between Saline and S-AMPA treated groups. Data is presented as means ± SEM; information about the presentation of the results and associated statistics are described in each figure legend.

2.3 Results

2.3.1 Verification of mouse anti-pERK antibody efficacy and specificity in wildtype zebrafish

Since this mouse phospho-ERK1/2 primary antibody has not been tested in zebrafish before, it was necessary to first determine if any immunoreactivity was detectable in the brain and pituitary tissue, and then establish baseline pERK levels in non-ovulating female fish. The pERK primary antibody was immunoreactive in zebrafish brain tissue and generated the strongest signal at a dilution of 1:200. pERK-immunoreactivity (ir) was observed dispersed throughout the brain, located in neurons and other cell types (possibly glial cells) throughout the olfactory bulb, telencephalon, hypothalamic nuclei, and pituitary cells (Fig 2.1 and 2.2). pERK-ir appears to be localized mainly in the cell bodies of neural cells, extending into cell processes. This staining reveals a level of baseline pERK expression.

The next step was to ensure it was possible to co-stain sections with primary antibodies for pERK and SNa. Females were again sampled and dissected in the afternoon, well outside their naturally occurring ovulatory window. Strong pERK immunoreactivity was observed in what appear to be cell processes extending down from hypothalamic nuclei through the hypophyseal stalk and into the pituitary. Additionally, pERK appears to be localized in cells in the rostral pars distalis (RPD), and proximal pars distalis (PPD), which are the locations of lactotrophs and gonadotrophs respectively (Fig 2.2). These results show this mouse pERK antibody as suitable for use on brain and pituitary tissue, and that it can be successfully used in conjunction with our SNa antibody to later investigate SNa neuron activation during ovulation.

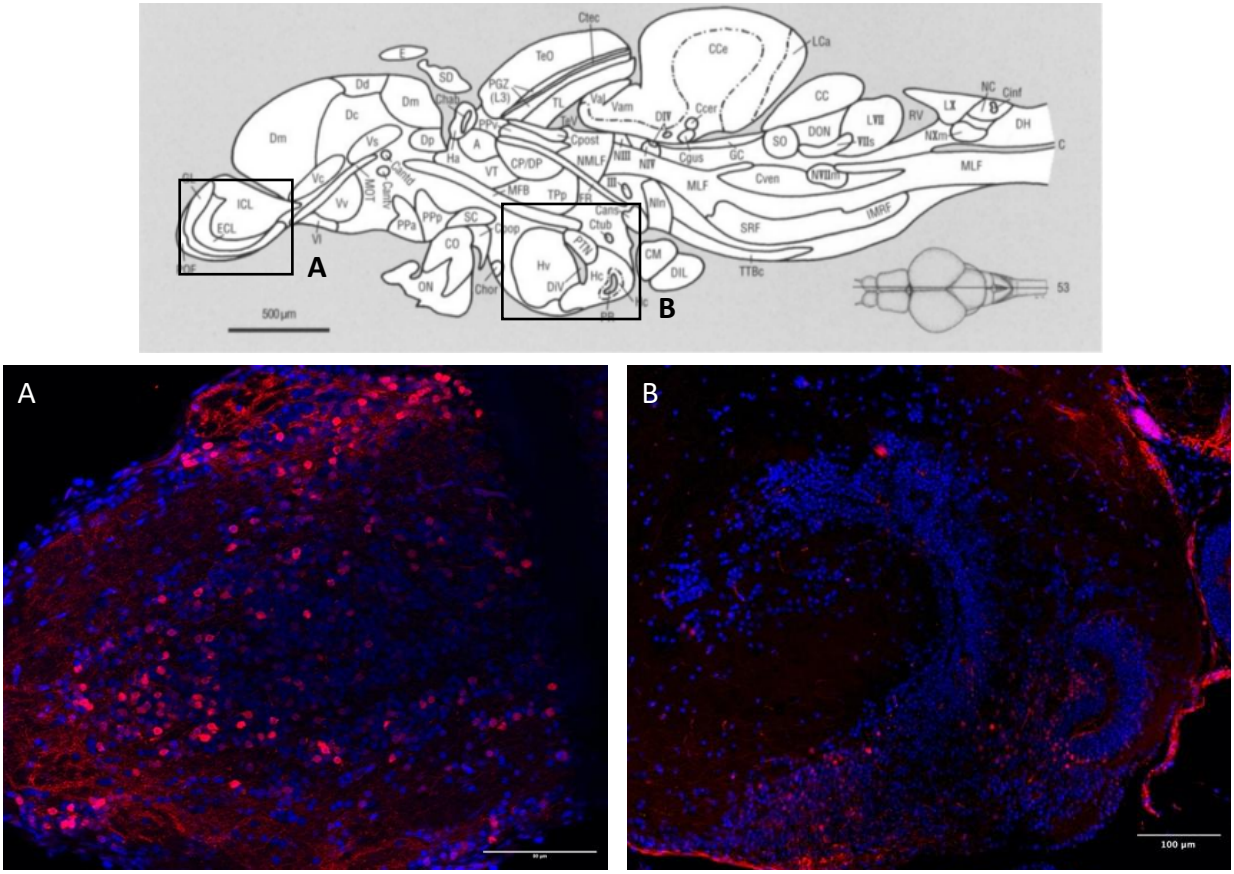

Fig 2.1 Baseline levels of phospho-ERK (pERK) immunoreactivity in zebrafish brain. pERK can be observed in zebrafish brain tissue using mouse anti-phosphoERK1/2 (Thr202, Tyr204) primary antibody (Catalog # 14-9109-82). In the **(A)** olfactory bulb and **(B)** hypothalamus, pERK is observed in a random distribution of neural cells. Red fluorescence labels pERK-ir, blue fluorescence labels cell nuclei.

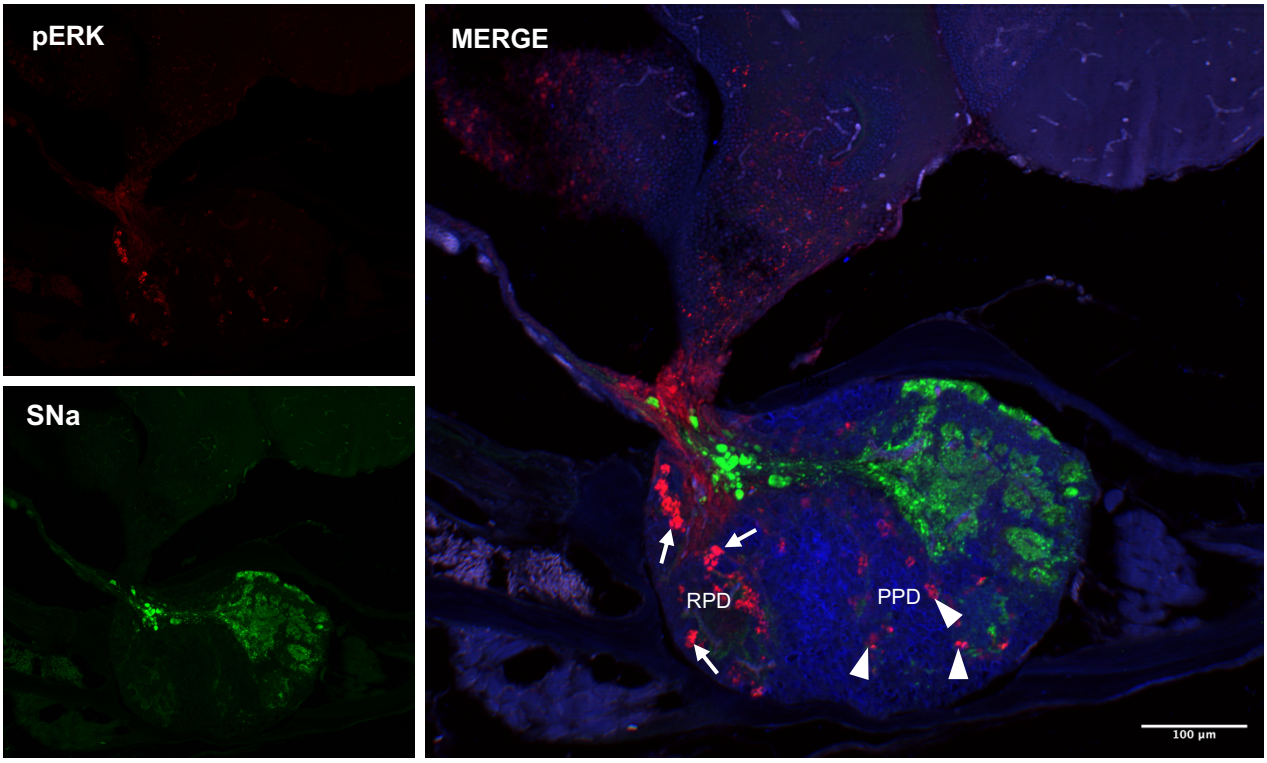

Fig 2.2. Phospho-ERK and SNa in non-ovulating zebrafish pituitary. Phospho-ERK immunoreactivity is observed in likely lactotroph cells in the rostral pars distalis (RPD) (arrows), and likely gonadotroph cells in the proximal pars distalis (PPD) (arrowheads). Nuclei are stained in blue. Samples were imaged using Zeiss Axio Imager Upright Fluorescence Microscope with Apotome.

2.3.2 Testing specificity by blocking immunoreaction with custom pERK peptide

To further confirm specificity of this antibody and validate its use in zebrafish, it is necessary to block the signal using pERK peptide. Pre-incubation of the primary antibody with the epitope peptide successfully blocked pERK immunoreactivity in adult brain tissue at 5 uM, 10 uM, and 15 uM of the peptide. Samples treated with normal regiment of 1:200 diluted primary antibody displayed the anticipated pattern of expression where pERK is observed throughout in the olfactory bulb, preoptic area, hypothalamus, and pituitary (Fig 2.3). Samples treated with primary antibody pre-absorbed with 15uM of the epitope peptide were indistinguishable from those treated with only blocking buffer and anti-mouse Alexa594 secondary antibody (Fig 2.3). The same was observed for all three concentrations of the epitope peptide tested (not shown); the only red signals detectable in these samples were autofluorescence present in blood vessels and membranes. This reveals that the mouse anti-phosphoERK1/2 (Thr202, Tyr204) monoclonal antibody specifically

binds to the double phosphorylated version of pERK (the fully active form of the protein). There appears to be little off-target binding or non-specific binding and thus, this antibody is potentially useful to study cellular activation in zebrafish brain and pituitary tissue.

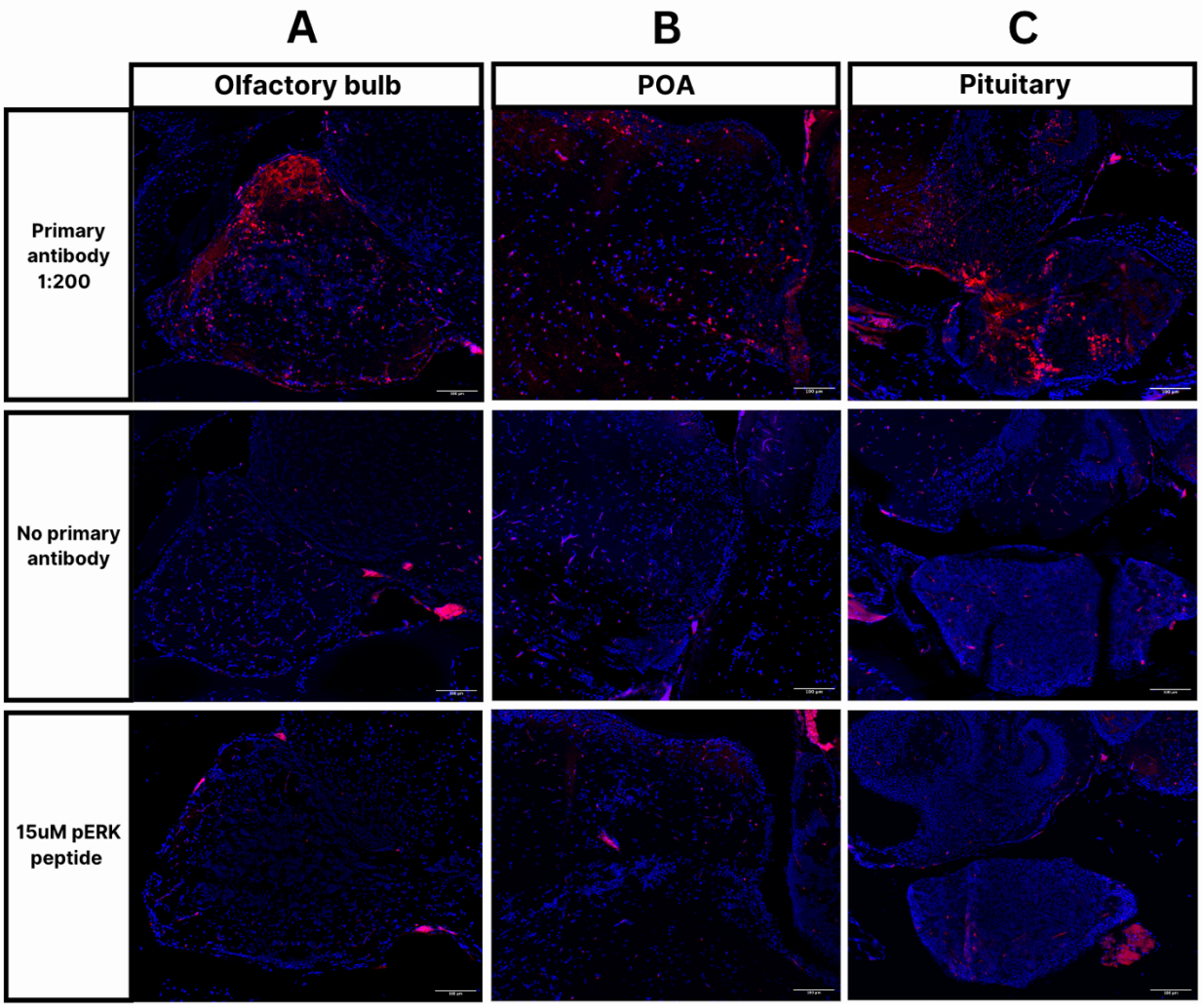

Fig 2.3. Confirming specificity by blocking immunoreaction with custom designed pERK peptide. Phospho-ERK immunoreactivity is blocked in the **(A)** hypothalamus, **(B)** preoptic area, and **(C)** pituitary upon pre-absorption of the primary antibody with 15uM pERK epitope peptide. Red fluorescence labels pERK-ir, blue fluorescence labels cell nuclei. Samples were imaged using Zeiss Axio Imager Upright Fluorescence Microscope with Apotome at 10X magnification.

2.3.3 Verifying pERK as suitable biomarker through glutamatergic activation

Prior to testing pERK and SNa localization during the ovulatory period, pERK must be verified as being an effective biomarker for true neuronal activation. The glutamate agonist S-AMPA was used to activate neurons in the adult female brain, to evaluate if there was a sufficient increase in pERK immunoreactivity following this stimulation, serving as a positive control.

Clear induction of p-ERK expression is observed within 3-minutes of intraperitoneal injection with S-AMPA in the hypothalamus of mature, non-ovulating female zebrafish. Though it appears that there is a considerable amount of pERK immunoreactivity observed in the pituitary of the S-AMPA injected sample, particularly in and around the rostral pars distalis (location of gonadotrophs) (Fig 2.4A) – the mean number of positive cells increased from 40 cells to 68 cells in the saline and S-AMPA groups respectively – the increase was not significant (Fig 2.4B; $n = 4$, $p = 0.0841$). Conversely, significantly more immunoreactivity can be observed in the lateral and periventricular hypothalamic nuclei of the S-AMPA injected fish compared to the saline injected control (Fig 2.4C). This is further shown quantitatively, as the mean number of pERK positive cells increase 1.67-fold from 344 to 574 cells in the saline and S-AMPA injected fish respectively (Fig 2.4D; $n = 4$, $p < 0.05$).

In the preoptic area, injection of S-AMPA significantly increased cell activation within 3 minutes in comparison to saline injected controls. The mean number of pERK positive cells in the POA significantly increased from 189 cells in the saline injected fish to 433 in those injected with S-AMPA, representing a 2.3-fold increase (Fig 2.5A; $n = 4$, $p < 0.05$). There is strong pERK immunoreactivity observed within pre-optic neurons, particularly those concentrated in the gigantocellular part of the magnocellular preoptic nucleus (PMg), magnocellular preoptic nucleus (PM), as well as increased levels of pERK in the posterior part of the parvocellular preoptic nucleus (PPp) in S-AMPA injected fish (Fig 2.5B). The preoptic nucleus is a very important location of SNa magnocellular neurons, the cell bodies of which are densely packed in the PM. Interestingly, it appears pERK immunoreactivity is localized in neurons and other cells that are in close proximity to these SNa magnocellular neurons, but not co-localized within the SNa-ir neurons themselves.

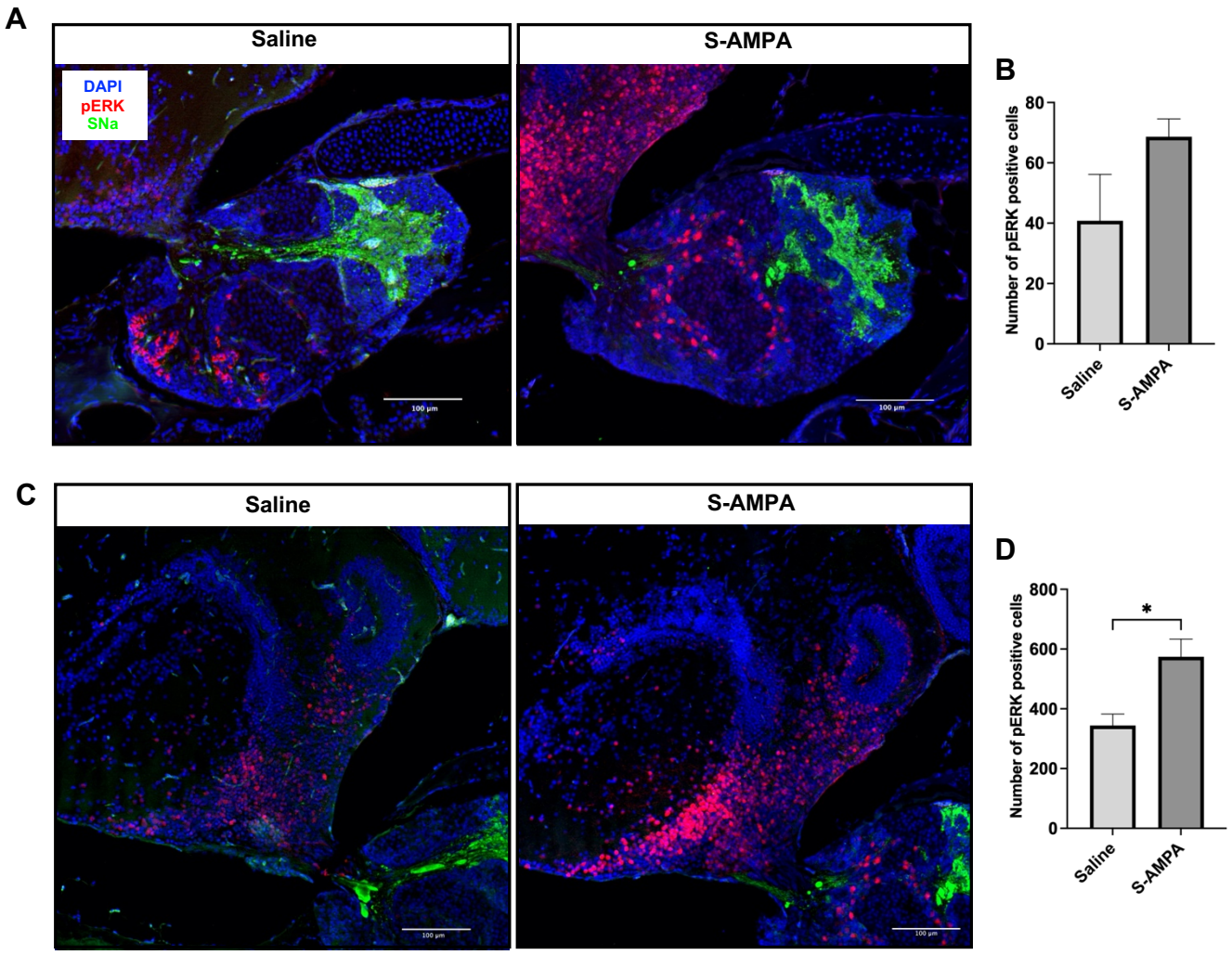

Fig 2.4. Phospho-ERK immunoreactivity 3 minutes after injection of wildtype females with saline or S-AMPA. **(A)** Distribution of phospho-ERK immunoreactivity and **(B)** the number of pERK positive cells in the pituitary (n = 4, p = 0.0841). **(C-D)** Phospho-ERK activity is increased in the lateral and periventricular hypothalamic nuclei following IP injection of S-AMPA. Values in B and D are reported as means + SEM (n = 4, $p < 0.05$). Green florescence labels SNa-ir, red florescence labels pERK-ir, blue fluorescence labels cell nuclei.

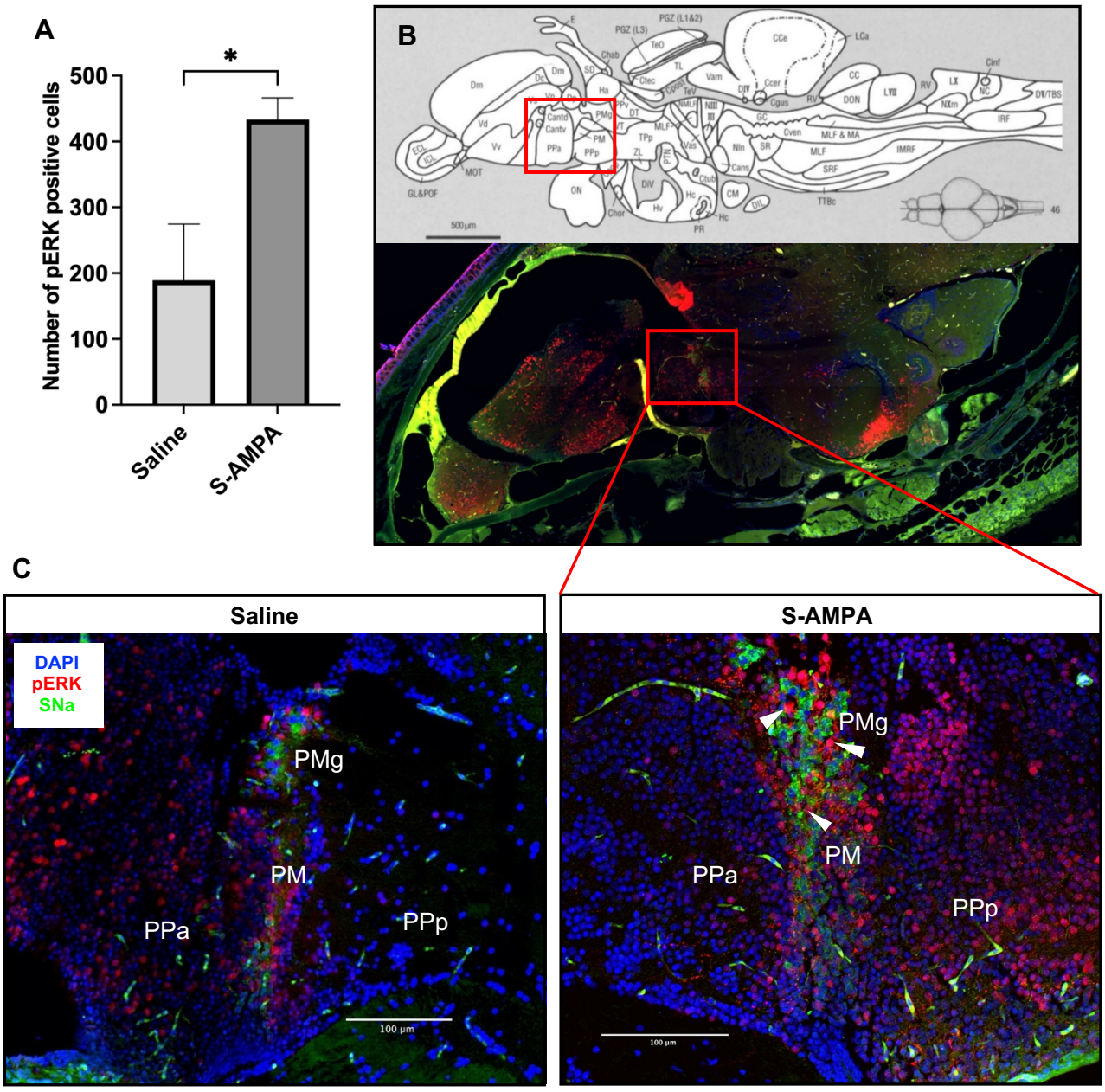

Fig 2.5. S-AMPA injection increases cell activation in the pre-optic area 3 minutes post-IP injection. (A) Results are reported as means + SEM. (n=4, $p < 0.05$, unequal variance t-test). **(B) (C)** Strong pERK immunoreactivity observed in the pre-optic neurons near, but not in the secretoneurin (SNa)-positive magnocellular neurons (arrowheads). Green florescence labels SNa-ir, red florescence labels pERK-ir, blue fluorescence labels cell nuclei.

2.4 Discussion

Here we demonstrated successful immunoreaction using a commercial mouse anti-phospho-ERK primary antibody in WT zebrafish neuroendocrine tissue. We also provide evidence of the effectiveness of this antibody at detecting transient cell activation with clear induction of increased pERK signal following stimulation of glutamatergic neuronal circuits, reinforcing specific brain regions as important centers of neuroendocrine control, and solidifying pERK as a suitable and reliable biomarker for neuronal activation. Utilizing biomarkers for neuron activation has been common practice to investigate neuronal circuits, and elucidate the functions of neuropeptides, neurohormones, and neurotransmitters (Cancedda et al., 2003; Gao & Ji, 2009; Randlett et al., 2015). To study activation of SNa neurons at different times across the ovulatory cycle, as well as observe anatomically which brain regions are active at targeted time points, immunohistochemistry is the most suitable method. Commercial pERK primary antibodies have been used in mammals (Søland et al., 2008; Yang et al., 2010; (Chang et al., 2017) and used in zebrafish (Altmieme et al., 2019; W. Zhang et al., 2022). However, these antibodies primarily have rabbit as the host species, conflicting with our rabbit-anti-goldfish SNa antiserum (E. Zhao, Basak, Crump, et al., 2006). Since this antiserum is the only antibody documented to successfully detect SNa immunoreactivity in zebrafish tissues, a non-rabbit pERK antibody is needed with extensive validation to ensure its proper use in zebrafish brain immunohistochemistry.

In these validation experiments, we aimed to determine the optimal conditions for utilizing the mouse-anti-phosphoERK1/2 (Thr202, Tyr204) monoclonal antibody. It was found that diluting this antibody 1:200 generates a strong signal, similar to the manufacturer's recommended dilution of 1:100. With the rise of antibody use for biomarker discovery and implementation in physiological and pharmacological research, the level of validation required has been debated in recent decades. There are no standardized guidelines for validating commercial antibodies, but tiers of validation have been discussed and established according to metrics such as tissue type, previous cited IHC literature, intended use of the antibody (WB, flow cytometry, IF/ICC, IHC), etc, and include recommended controls to accomplish the appropriate level of validation for publication (Bordeaux et al., 2010; Howat et al., 2014; O'Hurley et al., 2014). The antibody we chose had not been previously used in zebrafish but has been successfully tested through WB (Hermanowicz et al., 2021) and IHC specifically in human cells (Pestronk et al., 2019; Brechbuhl et al., 2020). The sequences or the targeted epitope for human, mouse, rabbit, and zebrafish ERK

are identical (Appendix 1). Thus, evaluating the antibody through IHC application, carefully comparing the consistency of staining to establish a signal/noise ratio, adjustment of the antibody dilution, and blocking of the target epitope in the target tissue with synthetic peptides are adequate.

We successfully blocked pERK immunoreactivity with increasing concentrations of a synthetic phosphorylated peptide corresponding to the amino acid sequence of the pERK epitope targeted by the primary antibody. Blocking experiments make it possible to reveal the level of background staining in the tissue of interest, while also demonstrating the level of specificity possible for that given primary antibody. Conservatively, blocking experiments aim to have the peptide concentration be between 10 and 100X higher than the working primary antibody dilution to ensure any available antibody will be captured. We found that pERK immunoreactivity can be completely attenuated when tissue is treated with pre-incubation of the primary antibody with 15 μM of peptide solution (10X more than the working primary dilution), and as little as 5 μM of blocking peptide solution, which is below the 10X minimum threshold. Since there was no pERK staining in any of the three brain regions when treated with no primary antibody at all, as well as treatment with all tested concentrations of blocking peptide, it can be concluded that then primary antibody is specific in only recognizing the conserved region of the phosphorylated (activated) ERK peptide in the zebrafish brain.

Providing evidence for the effectiveness of biomarkers through positive and negative controls is essential (Howat et al., 2014; O'Hurley et al., 2014). Stimulating the nervous system with the glutamate agonist S-AMPA served as the positive control. We observed rapid increases in the number of cells stained for pERK in the olfactory bulb, hypothalamus, POA, and pituitary when treated with S-AMPA compared to the saline injected negative controls. It is important to note that the POA is an essential location for vertebrate reproductive control, evident by results from electrical stimulation of this area in mammal and other teleost models. Electrical stimulation of the POA in the bluegill, *Lepomis macrochirus,* results in stimulation of various distinct courtship behaviours observed during mating (Demski & Knigge, 1971). Whereas targeted lesioning of the POA in male cats impairs copulatory behaviour and overall reproductive success (Hart et al., 1973). The POA contains numerous glutamatergic neurons that play important thermogenic roles in menopausal mice (Su et al., 2022) and control courtship in bluehead wrasses, *Thalassoma bifasciatum* (Luong et al., 2023). Together, the results of injecting the glutamate agonist S-AMPA verify pERK as a suitable biomarker for neuronal activation and highlight its

ability to detect changes in cell activation within a very short time span. This is essential for later evaluating the changes in cellular activation throughout different stages of the ovulatory cycle. Additionally, the outcome of this validation experiment highlights the hypothalamus, pituitary, and preoptic area as sensitive to glutamate action, and reinforce these regions as important areas of neuroendocrine control. Tracing time-dependent pERK expression with this phospho-ERK primary antibody and immunohistochemistry is the proposed strategy to identify key neuroendocrine neurons activated in the peri-ovulatory period (Chapter 3), and for pituitary cell activation following SNa injections (Chapter 4).

Chapter 3. Preoptic SNa magnocellular neurons are activated prior to ovulation

3.1 Introduction

In female vertebrates, ovulation is the process where oocytes mature and are released from ovarian follicles. Surge release of Lh is driven by hypothalamic Gnrh release which acts on gonadotrophs in the anterior pituitary (Goetz & Garczynski, 1997; Tsafriri & Reich, 1999; Ma et al., 2004; Kanda, 2019; Trudeau, 2021; Zohar et al., 2021). Absence of Lh following gene mutations disrupts ovulation and results in infertility in zebrafish and medaka (Takahashi et al., 2016; Z. Zhang et al., 2015), reinforcing the essential role of Lh in ovulation. The dynamic control of gonadotropin release through the brain-pituitary axis by Gnrh and many other neuropeptides and neurotransmitters is key for the timed regulation and success of teleost ovulation (Trudeau, 2021; Zohar et al., 2021). While many neuropeptides are implicated, essential neuropeptidergic circuits involved in the coordination of ovulation in fishes have mostly remained elusive.

In murine models, hypothalamic and preoptic populations of neurons releasing kisspeptin are activated in the periovulatory period, regulating the pulsatile release of Gnrh leading to the Lh surge and ovulation (Adachi et al., 2007; Christian et al., 2005). In mammals, oxytocin (Oxt) is associated with ovulation and stimulation of the Lh surge (Johnston et al., 1990; Melli et al., 2007), but little is known about the mechanisms involved. Isotocin (Ist) and arginine vasotocin (Avt), the fish homologs of the mammalian nonapeptides Oxt and arginine vasopressin (Avp) respectively, are important for social-sexual behaviour (Goodson & Bass, 2001; Mennigen et al., 2022a). The Oxt/Ist and Avp/Avt cell bodies are located in the teleost POA, projecting mainly to the pars nervosa, but also to the PPD of the pituitary where they may modulate Lh release (Canosa et al., 2011; Foran & Bass, 1998; Markham et al., 2019; Pouso et al., 2019; Scaia et al., 2022; Peng, 2022).

The periovulatory changes in Gnrh, Kp, Oxt, Lh and ovulation are tightly controlled by circadian rhythms in mammals (Sellix & Menaker, 2010). Daily light-dark cycles also control ovulatory cycles in teleost fishes (Aida, 1988; Blanco-Vives & Sánchez-Vázquez, 2009; Giannecchini et al., 2012). Females of many fish species exhibit serial spawning in which they complete a full ovulatory cycle within 24 to 96 hours (Migaud et al., 2010). In zebrafish, this cycle is 24 hours long, with ovulation happening near the end of the dark period (Blanco-Vives & Sánchez-Vázquez, 2009). In both male and female teleosts, the timed release of hormones and

pheromones leading up to and following the Lh surge promotes successful ovulation (Amagai et al., 2022). The neuroendocrine mechanisms underlying ovulatory cycles in teleosts have largely been assumed to be similar to mammals. However, critical evidence from gene mutation models challenges this. For example, mutation of both Gnrhs in zebrafish does not affect spawning (Zohar et al., 2021). Zebrafish harbouring mutations in the kisspeptins (Kp), and their receptors also spawn normally (Tang et al., 2015). Additionally, mutation of Oxt in medaka affects mate choice but does not disrupt spawning (Yokoi et al., 2020). Such observations have accelerated the search for new neuroendocrine regulators of reproduction.

In this regard, secretoneurin, a 31-34 amino acid neuropeptide generated by specific prohormone convertase processing of larger precursor protein secretogranin-2 (Scg2), has emerged as an important player in teleost reproductive control (Zhao et al., 2011; Mitchell et al., 2020; Trudeau, 2021). It is co-localized within preoptic Ist magnocellular neurons in goldfish (Canosa et al., 2011) and zebrafish (Peng, 2022), which project to the pituitary and are suggested to directly regulate Lh release (E. Zhao, Basak, & Trudeau, 2006). Whole brain levels of SNa in wildtype zebrafish have been documented to increase throughout the periovulatory period and peak around the presumptive Lh surge (Peng, 2022) while scg2a mutant zebrafish exhibit significant reproductive and ovulatory deficits (Mitchell, Zhang, et al., 2020). These include reduced expression of *gnrh3* in the hypothalamus, reduced *lhb* and *cga* in the pituitary. These results together highlight SNa as a neuropeptide potentially involved in ovulatory control, though activity of SNa neurons in the brain have not been investigated.

Taking advantage of the daily zebrafish ovulatory cycle, we tracked SNa neuron activation throughout the periovulatory period. Using the previously validated pERK primary antibody (Chapter 2), our data indicate that SNa neurons in the POA are progressively activated in the periovulatory period

3.2 Materials and methods

3.2.1 Experimental animal husbandry

Experimental WT zebrafish were kept and bred in the University of Ottawa aquatics room. Fish were maintained at 28˚C under a photoperiod consisting of lights-on from 0900h to 2300h and fed 2 times daily. All experiments followed animal use protocols generated under the guidelines of the Canadian Council on Animal Care and were approved by the University of Ottawa's Animal Care Protocol Review Committee.

3.*2.2 Ovulatory cycle sampling experimental design*

Mature wildtype 6-10 mpf females were used for this experiment. Classical breeding tanks were set up containing one male and one female separated by a divider and kept in a 28˚C incubator. Tanks were assigned to each of the following three sampling times: 2:00h, 05:00h, 08:30h.

There are several important previous observations that provide the basis for these periovulatory sampling times. Other groups have reported that at 02:00h (6 hours prior to lights on) *lhb* mRNA levels were highest (So et al., 2005); at 05:00h (3 hours prior to lights on) levels of Lh were highest (this is the time of the presumptive Lh surge), with ovulation occurring approximately at 08:30h (So et al., 2005; Tang et al., 2016). Following these, our lab performed simultaneous measurements of reproductive peptides in the whole brain and revealed that SNa and Gnrh3 are highest at 05:00h (Peng, 2022). At the time of sampling, experimental females were removed from the incubator and kept in the dark until dissection. Female fish were sacrificed using a cold shock in an ice bath. The skull flap was carefully removed to allow for better penetration of the brain tissue during tissue processing and placed in 4% paraformaldehyde for 24 hours for fixation. The same paraffin embedding protocol was followed as described in Chapter 2.2.4.

3.2.3 Immunofluorescence

Slides were heated on a slide warmer at 60˚C for 30 min and then deparaffinized using xylene twice for 20 min. Slides were then rehydrated using an ethanol (EtOH) series of decreasing ethanol concentrations for 10 min each (99% and 95% EtOH twice, 70% once), and finally in PBS for 10 min.

For antigen retrieval, slides were incubated with an antigen retrieval buffer of 0.01M Sodium Citrate (pH 6.0) in an 84-90˚C water bath for 30 min. Slides were removed, allowed to cool, washed 2X with PBS for 2 min before being treated in a blocking buffer (1% skim milk, 0.3% Triton-100) at room temperature for 30 minutes. For immunofluorescence, all slides were first incubated overnight at 4˚C with a validated rabbit-anti-goldfish SNa antiserum (Zhao et al., 2006) diluted 1:800, and validated mouse-anti-phosphoERK1/2 (Thr202, Tyr204) monoclonal antibody diluted 1:200 (Invitrogen, cat# 14-9109-82). The next day after being washed with 1xPBS, all slides were treated in the dark with Goat anti-Rabbit IgG (H+L) Cross-Adsorbed Secondary Antibody, Alexa Fluor™ 488 (Invitrogen, cat# A-11008) and Goat anti-Mouse IgG1

Cross-Adsorbed Secondary Antibody, Alexa Fluor™ 594 (Invitrogen, cat# A-21125), both diluted 1:500.

All slides were washed 2X with 1xPBS completely shielded from any light. Slides were treated with 50-60 µl of SlowFade™ Diamond Antifade Mountant with DAPI (Invitrogen, cat# S36973) and mounted with 22x60mm No. 1.5 coverslips (VWR, cat# 48393-221).

3.2.4 Cell counting and data collection

Samples were imaged using Zeiss Axio Imager.Z2 Upright Fluorescence Microscope with ApoTome.2. Serial images were taken of every other section on the slide, starting from the first section present. The POA was identified following (Wullimann et al., 1996) and images were taken from identical sites. All images were collected as Z-stacks, and then processed using the Extended Depth of Focus function in ZEN 3.2.0. Co-localization was determined using the 3D-reconstruction display (powered by Arivis) generated after taking the z-stacks. The brightness, contrast, and colour balance of each captured image were adjusted using FIJI in ImageJ.

For cell counting, a systematic random sampling strategy was applied (Geuna, 2000; Canosa et al., 2011). A 100 µm grid was applied to each image, and a set sample area was established for POA. A 4x3 grid was used as the sampling area (Fig 3.1). Positive pERK immunoreactive cells, SNa immunoreactive cells, and pERK&SNa immunoreactive cells (cell profiles) were counted with the determined grid. The total number of cell profiles was summed for each section, and the average number of cell profiles was established by dividing the sum of all cell profiles of a particular region by the number of sections analyzed for that fish. Images were coded and randomized by an independent party to minimize bias in counting.

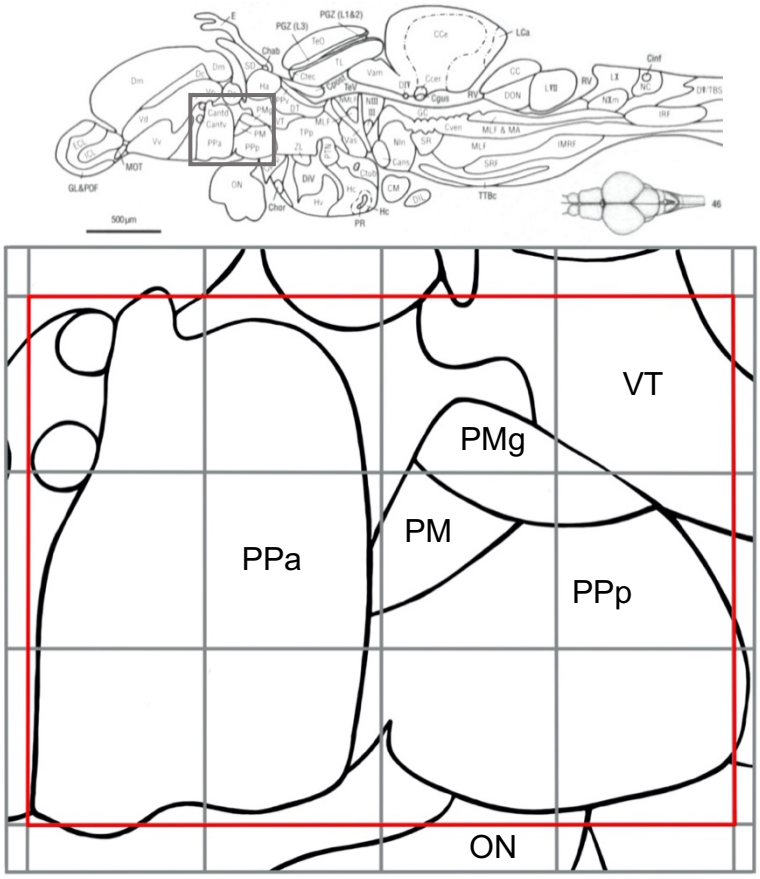

Fig 3.1. Schematic of POA cell counting method. A 100 x100 µm grid was applied to each image of POA captured at 20X magnification. The top diagram is an annotated schematic of a sagittal section of the whole zebrafish brain. The grey box represents the brain area represented in the bottom, zoomed in diagram. The red box is the sample area, only cells counted within the grid are represented in collected data. PPa, parvocellular preoptic nucleus, anterior part; PPp, parvocellular preoptic nucleus, posterior part; PM, magnocellular preoptic nucleus; PMg, gigantocellular part of the magnocellular preoptic nucleus; ON, optic nerve; VT, ventral thalamus.

3.2.5 Data and statistical analysis

Statistical analysis was performed using GraphPad Prism 9 Software (GraphPad Prism Inc.). Normality was tested for data collected for the number of positive pERK, SNa, pERK&SNa immunoreactive cells, and percentage of SNa cells that are pERK positive in the POA using the Shapiro-Wilk test. To test for significance between timepoints, normally distributed, parametric data sets were then analyzed using one-way ANOVA with Tukey post-hoc test, non-parametric data was analyzed using Kruskal-Wallis test with Dunn's multiple comparisons test. Parametric data is presented as means + SEM, nonparametric data is presented as medians; information about the presentation of the results and associated statistics are described in each figure legend.

3.3 Results

3.3.1 pERK expression in SNa -positive neurons in the POA

We visualized SNa and pERK immunoreactivity in the POA of female fish at different time points to map SNa neuron activity in the periovulatory period. For the first time we observed pERK-ir in SNa positive cells (Fig 3.2 & 3.3). In pERK positive cells, there is clear, strong staining observed localized in the nucleus, and in some cells also some diffuse staining throughout the cytoplasm (Fig 3.2C); the cytoplasmic pERK staining is more mutated and diffuse than nuclear staining (Fig 3.2C). This is in accordance with the main function of pERK as a nuclear kinase with a wide variety of transcription factor substrates (Chen et al., 1992; Kato et al., 1995), while a small portion of activated ERK is maintained in the cytoplasm (Wortzel & Seger, 2011). Cells that are negative for pERK staining have no nuclear staining or no cytoplasmic staining (Fig 3.2C & 3.2D). SNa is localized solely to the cytoplasm and cell processes (Fig 3.2B and Fig 3.3B). There is a distinct difference observed between SNa positive neurons that are also pERK positive and those that are negative. There is neither detectable pERK staining in the nucleus nor even mild staining in the cytoplasm (Fig. 3.2D). Most pERK-positive cells throughout the entire POA are not positive for SNa. pERK-ir is strongest overall in the center of the gigantocellular part of the magnocellular preoptic nucleus (PMg) and extending down into the magnocellular preoptic nucleus (PM) (Fig 3.3C), with strong nuclear expression of pERK observed extending into the cells localized in the anterior part of the parvocellular preoptic nucleus (PPa), and less overall in the posterior part of the parvocellular preoptic nucleus (PPp) (Fig 3.3C).

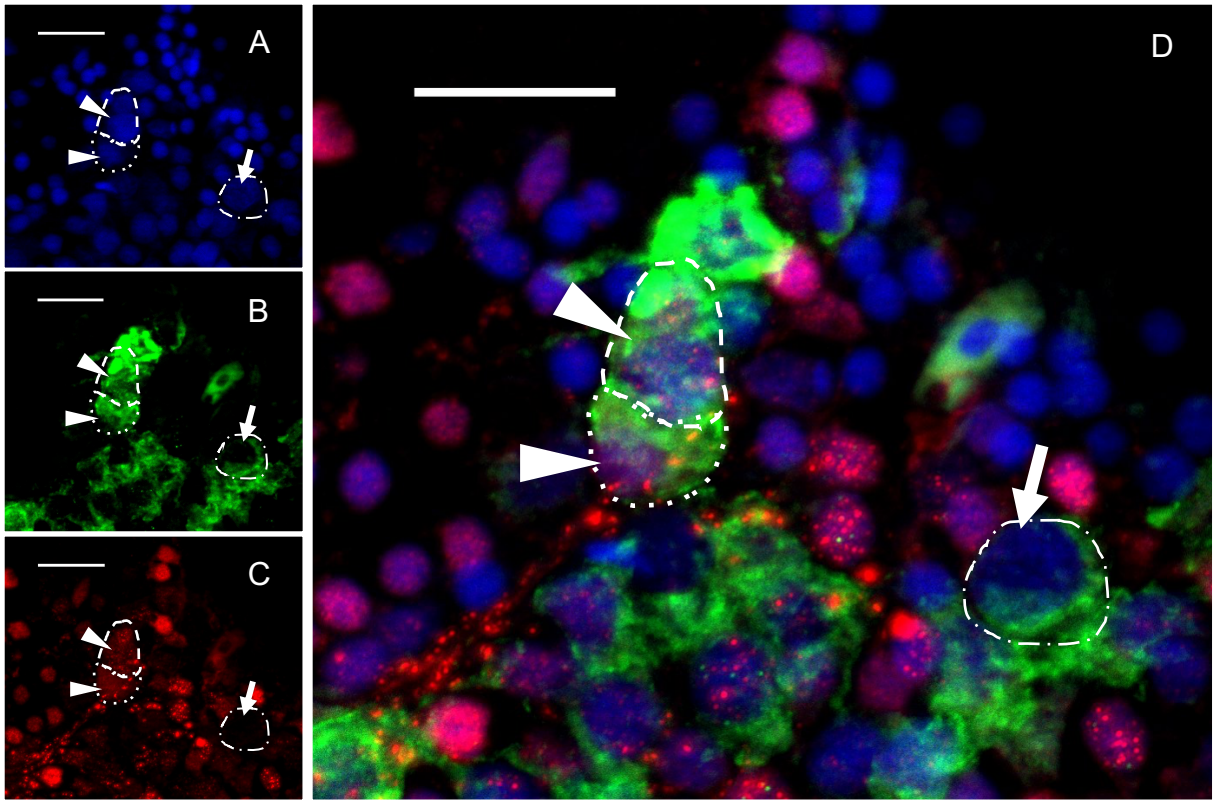

Fig 3.2. Positive pERK immunoreactivity in POA neurons. (A) Immunolabelling for nuclei with DAPI (blue). **(B)** Immunolabelling for SNa (green). **(C)** Immunolabelling for pERK (red). **(D)** Merge of (A-C). Each different pattern dotted line represents an individual SNa positive cell. Arrow heads are indicating SNa and pERK double immunoreactive cells. Arrow is indicating a SNa positive cell that is not pERK positive. Magnification 40X, bar scale is 20µm. Image also included in Fig 3.3.

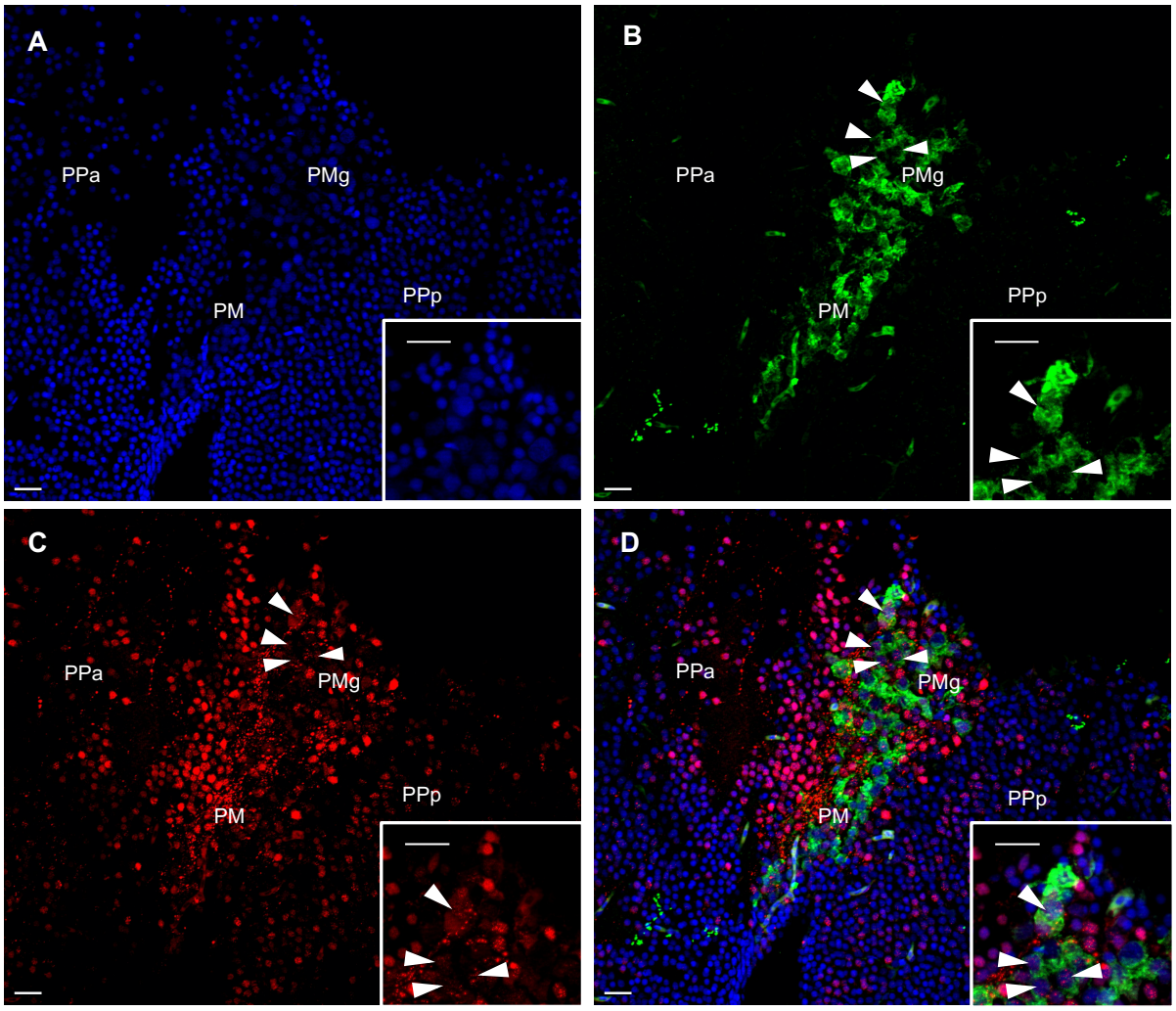

Fig 3.3. SNa magnocellular neuron activation in the POA at the time of presumptive ovulation (8:30h). (A) Immunolabelling for DAPI (blue). **(B)** Immunolabelling for SNa (green). **(C)** Immunolabelling for pERK (red). **(D)** Merge of **(A-C).** Arrowheads in all panels and insets indicate activated SNa-positive magnocellular neurons. Magnification is 20X (40X for insets), bar scales for (A-D) including insets are 20µm.

3.3.2 SNa neuron activity increases leading up to ovulation

There was no effect of time on the total numbers of SNa cell bodies (Fig 3.4A; n = 4, (F) = 0.0211, p = 0.979) or pERK immunoreactive cells in the POA (Fig 3.4B; p = 0.9410). In contrast, there was a progressive increase in activated pERK-positive SNa neurons in the periovulatory period (Fig 3.4C; (F) = 5.556, $p < 0.05$). There was a 1.61-fold increase in mean number of activated SNa neurons from 2:00h to 5:00h (p = 0.3621) and a 1.9-fold increase from 5:00h to 8:30h (Fig 3.4B; p = 0.0941).

SNa neurons are most active at 8:30h (Fig 3.4G), and there is a significant 3.1-fold increase of the mean number of activated pERK-positive SNa neurons from 2:00h to 8:30h (Fig 3.4B, $p < 0.05$). Additionally, the percentage of total SNa neurons that were active significantly increased in the periovulatory period (Fig 3.4D; $(F) = 9.043$, $p < 0.01$), specifically from 2:00h to 8:30h (Fig 3.4C, $p < 0.01$), as well as 5:00h to 8:30h (Fig 3.4C, $p < 0.05$). The mean percentage of SNa neurons activated were 6.9%, 9.9%, and 21.0% for 2:00h, 5:00h, and 8:30h, respectively (Fig 3.4C).

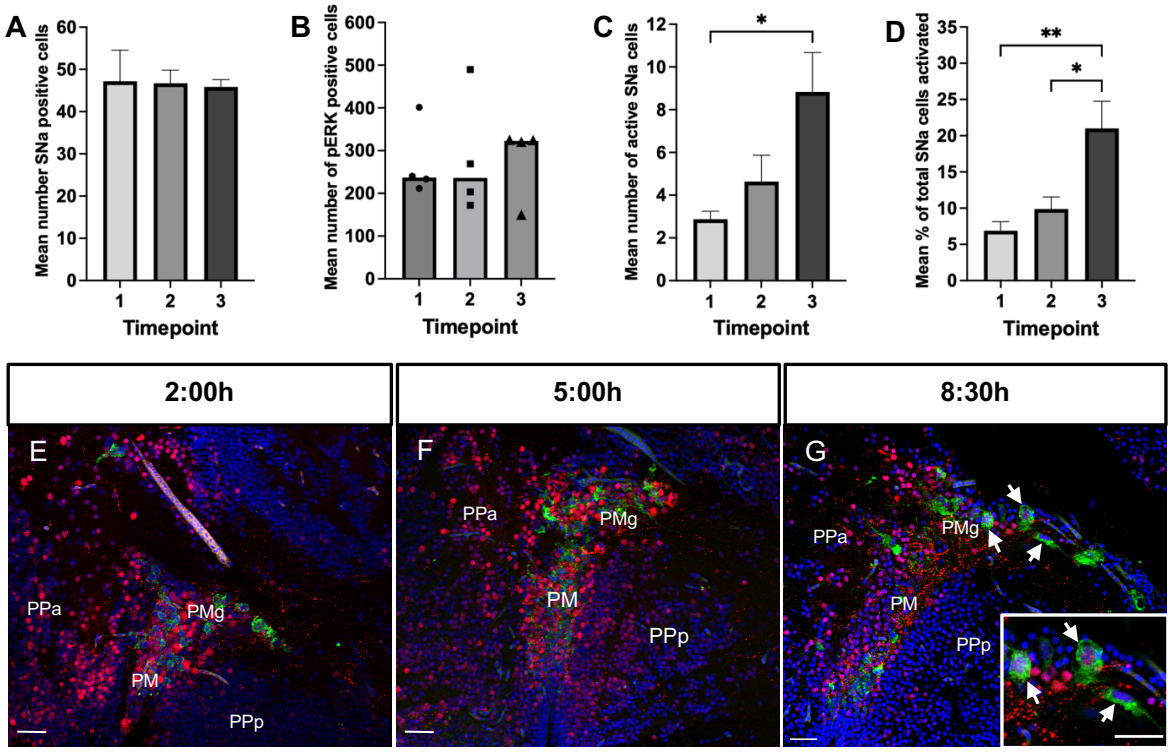

Figure 3.4. The number of active SNa neurons increases leading up to the time of presumptive ovulation. The time points represent (1) 2:00h, (2) 5:00h, and (3) 8:30h for **(A)** mean number of SNa positive cells, **(B)** mean pERK positive cells, **(C)** mean number of active SNa cells, and **(D)** mean percentage of total SNa cells activated, in the POA. Results in A, C, & D are presented as means +SEM, results in B are presented as medians; * denotes $p < 0.05$, ** denotes $p < 0.01$. SNa (green) and pERK (red) immunoreactivity at **(E)** 2:00h, **(F)** 5:00h, and **(G)** 8:30h in the POA. Arrows indicate activated SNa neurons (immunoreactive for SNa and pERK). Nuclei are stained with DAPI (blue). Magnification of (E-G) is 20X, (G) inset is 40X. Bar scales for all panels including (G) inset is 20µm.

3.4 Discussion

In this study, the neuronal activation biomarker phospho-ERK was visualized with SNa in the POA at 2:00h, 5:00h, and 8:30h to assess the periovulatory change in SNa neuron activation. These results revealed the first demonstration that SNa neurons are activated prior to ovulation in a female vertebrate and provide insight into the spatial and temporal activity of SNa in the brain.

SNa is emerging as a major player in the control of teleost reproduction (Zhao et al., 2009; Trudeau et al., 2012; Mitchell et al., 2020). Targeted mutations in *scg2a* result in impairments of zebrafish reproductive behaviour and major deficits in ovulation (Mitchell, Zhang, et al., 2020). In vertebrates, the POA is a major neuroendocrine center, regarded as a hypophysiotropic reproductive control center. Large magnocellular neurons located within the PM and PMg of the goldfish and zebrafish POA express *scg2a* and are immunoreactive for SNa (Canosa et al., 2011; Peng, 2022). Magnocellular and paracellular cells in rats express *scg2* and are found to be expressed in a small subset of vasopressin expressing neurons (Ang et al., 1997). In fish, activation of the POA is important in mating behaviour. As in the present study, physical separation of zebrafish breeding pairs overnight preceding a mating aggression test led to increased cell activation in the PPa and PM of females (Scaia et al., 2022a). Aggression and mate choice are involved in the social behaviour network (SBN) encompassing reproduction and sexual behaviour, reinforcing the importance of the POA and cellular activation of this region during key reproductive events. These are also two of the same locations where we document strong pERK expression and strong, consistent SNa neuronal staining at all timepoints. The PM is a main location where we observed the increased activation of SNa neurons progressively through the periovulatory period, further highlighting preoptic SNa as an important source of overall SNa in zebrafish reproduction.

There was a progressive increase in preoptic SNa neuron activation through the periovulatory period, reaching the highest level at 8:30h, the time around which ovulation is presumed to occur, and when the females are preparing for spawning. Previous work examining the same three periovulatory timepoints found whole brain SNa and Gnrh3 were the highest at 5:00h, with peptide levels at 8:30h returning to match those observed at 2:00h (Peng, 2022). This aligns with the well-established importance of hypothalamic Gnrh stimulating the Lh surge necessary for successful vertebrate ovulation. In the goldfish pituitary, SNa is regulated by Gnrh to promote Lh secretion (Samia et al., 2004). Therefore, we predicted activation of preoptic SNa

neurons would be highest at 5:00h. Prior to this time, at 02:00h ~6.9 % of POA SNa neurons were also immuno-positive for pERK. This increased to 9.9% when we expected the Lh surge to be occurring (5:00h). Activation continued as time progressed closer to ovulation. At 08:30h, 21.0% of SNa neurons detected in the POA were active. This pattern of activation does not match with predictions. However, the previous reporting of SNa levels were from whole brain analysis, whereas we observed activation of a subset of SNa cells in the brain for the first time. Though overall levels of SNa in the brain may increase closer to when we expect the surge of Lh to be occurring, SNa activity may be dynamic throughout the periovulatory period, with specific SNa populations being more active than others, akin to the way Kp neuron activity is specific based on their hypothalamic locations (Brock & Bakker, 2013). Mapping the activation of these magnocellular SNa neuron populations at shorter intervals, for example hourly between 5:00h and 8:30h, may provide better temporal resolution of cellular activity. The results provide support at the cellular level for previous demonstrations of SNa peptide levels increasing within the periovulatory window. The progressive increase in SNa neuron activation observed in this study indicates temporal engagement of POA neurons before ovulation.

The activation of neuropeptidergic neurons prior to ovulation has also been observed in other vertebrate models. As the well-known master controller of the HPG axis and vertebrate reproduction, the activity of Gnrh neurons has been investigated extensively. Mouse Gnrh neurons in the POA exhibit increased firing activity in the afternoon compared to the morning when treated with high levels of estrogen and demonstrate activity patterns indicative of positive feedback (Christian et al., 2005). In mice and other rodents, the Lh surge is initiated by an increase in circulating estrogens, typically occurring in the afternoon, from the ovary that positively feedback to Kp neurons to regulate and increase Gnrh neuron firing (Adachi et al., 2007; Oka, 2023). Continuous infusion of the POA with anti-kisspeptin monoclonal antibodies blocks and decreases Lh release in rats (Adachi et al., 2007). Other groups have tracked the neuron activation biomarker c-fos, demonstrating activation of rat Kp neurons following injection of E2 (Adachi et al., 2007). Increased activation of hypothalamic neurons has been observed in response to initiation of copulatory behaviour by male mice, with approximately 30% of Kp neurons in the RP3V (rostral periventricular area of the third ventricle) showing consistent, strong c-fos staining. Acute ablation of RP3V Kp neurons decreased female copulatory behaviour and significant decreases in c-fos/Kp co-labelling (Hellier et al., 2018). Gnrh and Kp neurons in the hypothalamus and preoptic area are

activated within the periovulatory window, similar to our observations of SNa in POA. Compared to our results, these other neuropeptides appear to be activated leading up to the Lh surge, not as close to ovulation as preoptic SNa in the female zebrafish. It will be important to determine the activational sequence of SNa neurons in specific subdivisions of the POA in relation to activation of Gnrh and other systems during the periovulatory period.

Preoptic SNa neurons project to the pituitary. It is known that SNa can independently stimulate Lh release in mouse LβT2 gonadotrophs (E. Zhao et al., 2011) and dispersed goldfish pituitary cells (E. Zhao, Basak, & Trudeau, 2006). Quantification of pituitary periovulatory SNa levels revealed the highest detectable peptide amounts at 2:00h and 5:00h, significantly dropping closer to ovulation (Peng, 2022) and thus corresponding to the hypothesis that SNa is involved in stimulation of the Lh surge. Knowing that 7-20 % of POA SNa neurons are active in some capacity during the periovulatory period, we wanted to turn focus to the pituitary and the activation of Lh-secreting gonadotrophs. This will be presented in Chapter 4 and will provide evidence that injection of SNa stimulates major reproductive processes in female zebrafish.

Chapter 4. Intraperitoneal injection of SNa activates pituitary Lh cells in ovulating female zebrafish

4.1 Introduction

For female vertebrates, ovulation is the process whereby oocytes undergo maturation and release from ovarian follicles. This process is stimulated by a dynamic combination of hormones and peptides that induce important morphological changes driving successful ovulation (Espey, 1980; Espey & Richards, 2006). The Lh surge is the hallmark of ovulation, an indispensable step in the induction of follicular cells to produce ovarian-maturation hormone and progressing oocyte maturation (Aizen et al., 2018). Without Lh, zebrafish and medaka models display infertility, thus reinforcing the importance of the Lh surge in ovulatory success (Zhang et al., 2015; Takahashi et al., 2016). Surge release of Lh is stimulated by a multitude of hypophysiotropic hormones typified by Gnrh (Trudeau, 2021; Zohar et al., 2021; Casteel & Singh, 2022). However, previous studies have suggested the involvement of SNa, a 31-34 amino acid neuropeptide, in the HPG axis (Mitchell et al., 2020; Peng, 2022).

The results we have presented in Chapter 3 demonstrate that SNa neurons in the POA are activated prior to ovulation in female zebrafish. The activity of these neurons progressively increases throughout the periovulatory period, showing highest activation around the time of presumptive ovulation. This first demonstration of temporal SNa activity in the brain strengthens the hypothesis that SNa is acting within the reproductive axis to modulate reproduction (Chapter 3). Preoptic SNa neurons project to the pars nervosa of the pituitary (Canosa et al., 2011; Peng, 2022) and also to the proximal pars distalis (PPD), with SNa fibers terminating around gonadotrophs (Peng, 2022). Here we now turn our focus to the pituitary, to determine potential actions of SNa on gonadotrophs. We visualized pituitary pERK staining following SNa i.p injections of a *lhb-RFP;fshb-eGFP* transgenic line. Furthermore, the ovulatory status was analyzed following injection to replicate and advance observations reported by Peng (2022).

4.2 Materials and Methods

4.2.1 Experimental animal husbandry

The individual *lhb*-RFP and *fshb*-eGFP single transgenic lines were generously received from Dr. Berta Levavi-Sivan at the Hebrew University of Jerusalem (Golan et al., 2014). A double transgenic line was generated in our lab by crossing the two lines (Peng, 2022). The double transgenic line was used for the following experiments. Experimental zebrafish were bred and

housed in the University of Ottawa aquatics facility. Fish were maintained in the rooms at 28˚C under a consistent photoperiod consisting of lights-on from 9:00h to 23:00h. They were fed twice daily by Animal Care and Veterinary Staff. All experiments using zebrafish followed animal use protocols generated under the guidelines of the Canadian Council on Animal Care and were approved by the University of Ottawa Animal Care Protocol Review Committee.

4.2.2. Intraperitoneal injection of SNa and ovulation assay

To synchronize their reproductive cycles, 36 females aged 10 mpf were separated from males two weeks prior to the injection experiment. On the day of injection, females were randomly assigned to one of three housing tanks, and then using a random number generator were assigned to one of four experimental groups (n = 12): Saline, Low SNa, High SNa, and hCG. Females were anesthetized with 4.2% tricaine methanesulfonate solution before being injected intraperitoneally with either 0.6% NaCl (pH=7; 10 µl/g body weight), Low SNa (1 nmol/g body weight, or 4 µg/g body weight), High SNa (2.5 nmol/g body weight, or 10 µg/g body weight) or the Lh analog hCG (50 IU/g body weight) using a 32-gauge needle attached to a 10µl Hamilton syringe. Injections were performed between 10:00h and 12:00h. hCG was used as a positive control for the induction of ovulation, as it acts at the level of the gonads. Fish were returned to individual static tanks to recover, and then were sacrificed on ice 6 hours post injection. hCG can stimulate ovulation 3 hours post injection (Tang et al., 2016). The 6-hour time point was chosen based on previous experiments that showed ovulation occurs successfully 6 hours post injection of SNa and hCG (Peng, 2022). We wanted to assess the ability of a single i.p. injection of SN to activate pituitary Lh cells in relation to ovulation. Following injection, brains were dissected and placed in 4% PFA for immunohistochemistry (Chapter 2.2.4), and their ovaries dissected out to analyze ovulatory status. This was done by incubating the dissected ovaries in modified Cortland's medium to weaken the follicular layer and oocyte attachment (Tse & Ge, 2010). The number of ovulated and non-ovulated eggs were counted for each individual.

4.2.3 Paraffin embedding and immunofluorescence

Procedures reported in Chapter 2.2.4 were followed for paraffin embedding of the post-SNa injection dissected head samples. For immunohistochemistry analysis, only non-ovulated fish were chosen for the saline group, and only ovulated fish were chosen for the Low and High SNa groups. On the day of immunofluorescence treatment, all chosen slides were heated on a slide

warmer at 60˚C for 30 min and then deparaffinized using xylene twice for 20 min. Slides were then rehydrated using an ethanol (EtOH) series of decreasing ethanol concentrations for 10 min each (99% and 95% EtOH twice, 70% once), and finally in PBS for 10 min.

For antigen retrieval, slides were incubated with an antigen retrieval buffer of 0.01M Sodium Citrate (pH 6.0) in an 84-90˚C water bath for 30 min. Slides were removed, allowed to cool, washed 2X with PBS for 2 min before being treated in a blocking buffer (1% skim milk, 0.3% Triton-100) at room temperature for 30 minutes.

For immunofluorescence, all slides were first incubated overnight at 4˚C with validated mouse-anti-phosphoERK1/2 (Thr202, Tyr204) monoclonal antibody diluted 1:200 (Invitrogen, Cat# 14-9109-82). The next day after being washed with 1xPBS, all slides were treated in the dark with Goat anti-Mouse IgG (H+L) Cross-Adsorbed Secondary Antibody Alexa Fluor™ 647 (Invitrogen, cat #A21235) diluted 1:500. All slides were washed 2X with 1xPBS completely shielded from any light. Slides were treated with 50-60 µl of SlowFade™ Diamond Antifade Mountant with DAPI (Invitrogen, cat# S36973) and mounted with 22x60mm No. 1.5 coverslips (VWR, cat# 48393-221).

4.2.4 Cell counting and data collection

Samples were imaged using Zeiss Axio Imager.Z2 Upright Fluorescence Microscope with ApoTome.2. This fluorescent scope uses a Colibri 5/7 multicolor light source. To visualize *lhb*-RFP expression, a 555 nm excitation filter was used. For EGFP a 475 nm excitation filter was used; however, we discovered the EGFP signal to be too weak to image, therefore imaging proceeded without including *fshb*-EGFP expression. To visualize pERK and DAPI staining, 630 nm and 385 nm excitation filters respectively were used. Serial images were taken of every other section on the slide, starting from the first section present per slide. All images were collected as Z-stacks, and then processed using the Extended Depth of Focus function in ZEN 3.2.0. Co-localization was determined by using the 3D-reconstruction display (powered by Arivis) generated after z-stack sampling. The brightness, contrast, and colour balance of each captured image were adjusted using FIJI in ImageJ.

For cell counting, a systematic random sampling strategy was applied, adapted from Canosa et al. (2011) which was adapted from the methodology outlined by Geuna, 2000. Positive pERK immunoreactive cells, *lhb*-RFP-expressing cells, and pERK&*lhb*-RFP double positive cells (cell profiles) were counted in whole pituitary sections. The total number of cell profiles was

summed for each whole section, and the average number of cell profiles was established by dividing the sum of all cell profiles of a particular brain region by the number of sections analyzed for that fish. Images were coded and randomized by an independent party to minimize bias in counting.

4.2.5 Statistical analysis

Statistical analyses were performed using GraphPad Prism 9 Software (GraphPad Prism Inc.). Data collected for the number of pERK, pERK&*lhb*-RFP positive pituitary cells were determined to be normally distributed through the Shapiro-Wilk test. Data for the number of *lhb*-RFP cells was non-parametric. The Z-scores for 2 proportions using a one-tailed hypothesis were calculated for all pairwise comparisons. The null hypothesis (H_0) tested is that there is no difference in the number of pERK positive cells, *lhb*-RFP-expressing cells, and/or pERK&*lhb*-RFP positive cells between treatments. The data for the percentage of eggs ovulated was determined to be non-parametric and was subsequently analyzed through Kruskal-Wallis test followed by Dunn's multiple comparisons test. Parametric data are presented as means + SEM, non-parametric data are presented as medians. Other details concerning the presentation of the results and associated statistics are described in each figure legend.

4.3 Results

4.3.1 IP Injection of SNa stimulates activation of Lh gonadotrophs in the pituitary

In effort to further elucidate the relationship between SNa and gonadotroph activity during ovulation, we injected different doses of SNa into mature, isolated females to investigate the activation of the Lh-specific gonadotrophs. There was no difference in the mean number of pERK-positive cells throughout the pituitary between the three injected doses (Fig 4.1A, $n = 4$, $(F) = 2.052$, $p = 0.185$), nor was there an overall increase in the mean number of Lh gonadotrophs (Fig 4.1B; $p = 0.557$). Injection of SNa activated Lh gonadotrophs in the pituitary (Fig 4.1C, $(F) = 6.922$, $p < 0.05$). In the saline controls, it was observed that on average only one *lhb*-RFP cell was also pERK positive 6 hours following injection. There was a 2.57-fold and 2.41-fold increase between the Saline and Low SNa ($p = 0.575$), and Low SNa and High SNa ($p = 0.070$) respectively, though neither reached statistical significance (Fig 4.1C). In contrast, there was a striking 5.44-fold increase in the mean number of activated Lh cells observed between the Saline and High SNa injected group 6 hours post-injection (Fig 4.1C, $p < 0.05$).

In all treatment groups, non *lhb*-RFP expressing pERK stained cells are evident mainly neighbouring the Lh gonadotrophs. There are some pERK positive cells in the saline injected fish, contained within the PPD (Fig 4.2A, second panel). The same pattern of pERK staining is observed in the Low SNa (Fig 4.2B, second panel) and High SNa (Fig 4.2C, second panel) pituitaries, with pERK cells localized primarily in the PPD. Positive pERK staining is strongest in the nucleus of the cells, with diffuse staining throughout the cytoplasm (Fig 4.2D), matching expression patterns previously observed in other cell types (Chen et al., 1992; Wortzel & Seger, 2011; Chapter 2 and Chapter 3). Lh cells are found in clusters throughout the PPD (Fig 4.2B & 4.2C, third panels), with *lhb*-RFP expression observed throughout the cytoplasm and slightly stronger expression observed in the nucleus of most cells (Fig 4.2E). Activated Lh cells, in all treatments but most notably in the High SNa injected fish, are primarily found in the PPD (Fig 4.2C, fourth panel), and show strong nuclear pERK staining in the *lhb*-RFP-expressing cells (Fig 4.2F).

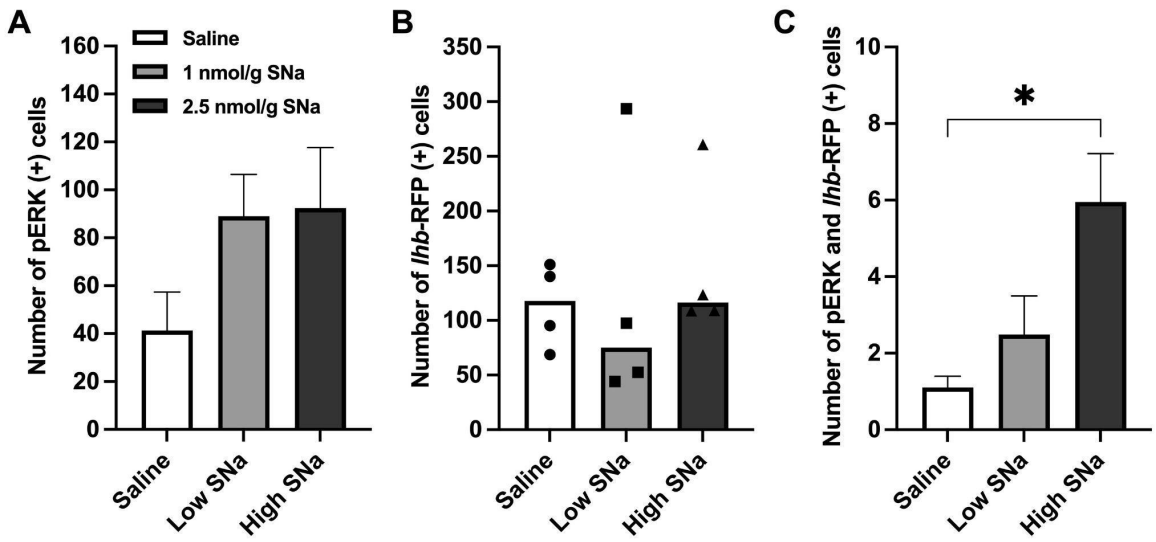

Fig 4.1. Whole pituitary cell counts 6 hours post SNa injection in *lhb*-RFP transgenic female zebrafish. (A) Number of pERK positive cells in the pituitary. **(B)** Number of *lhb*-RFP positive cells. **(C)** Number of activated *lhb*-RFP cells (*lhb*-RFP expressing and pERK positive). Data in A and C are presented as means + SEM, (n = 4), significance denoted by * (Tukey's multiple comparison test; $p < 0.05$). Data in B is presented as individual data points with medians (Kruskal-Wallis test with Dunn's multiple comparisons test; $p > 0.05$). Low SNa: 1 nmol/g; High SNa: 2.5 nmol/g.

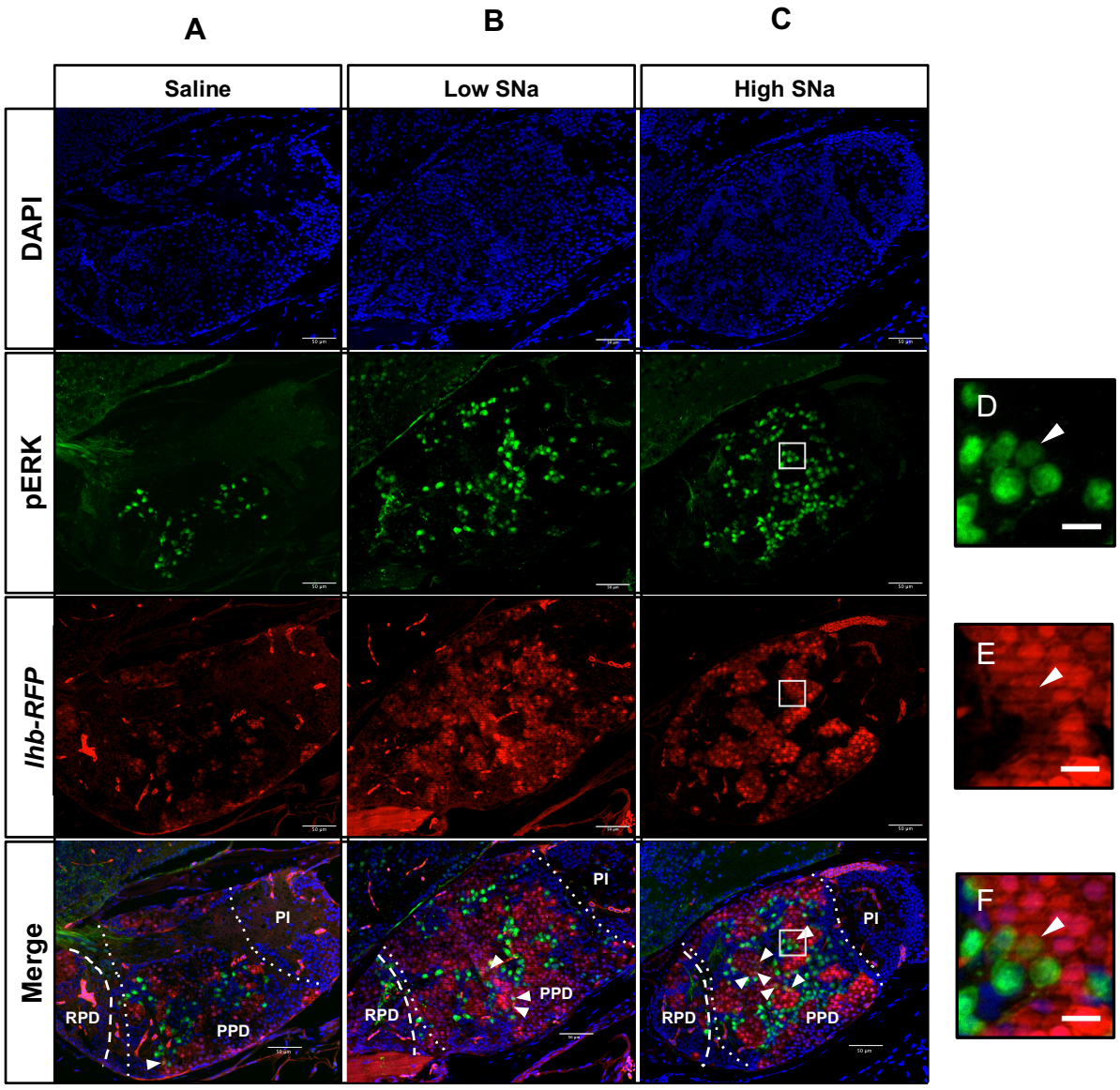

Fig 4.2. Fluorescence labelling of pERK and *lhb*-RFP expressing cells in female pituitaries following injection of SNa doses. (A) Immunolabelling for Saline, **(B)** Low SNa (1 nmol/g), **(C)** High SNa (2.5 nmol/g) injected fish, with DAPI in blue, pERK in green, *lhb*-RFP expression in red, and merged image with all channels. White boxes represent insets of **(D)** pERK staining, **(E)** *lhb*-RFP expression, and **(F)** Merged image of High SNa pituitary. Arrowheads indicate activated *lhb*-RFP cells (pERK positive). Dashed lines separate different pituitary regions. RPD, rostral pars distalis; PPD, proximal pars distalis; PI, pars intermedia. Scale bars in all panels of A-C are 50µm. Scale bars of D-F insets are 10µm.

4.3.2 IP injection of SNa stimulates ovulation in females isolated from males

The stimulation of Lh cells in the pituitary following SNa injection indicates that Lh secreting cells are activated. Given that the Lh surge drives ovulation, the effects on ovulation was also determined (Fig 4.3). In the saline injected group, 3 out of 12 of the fish ovulated (25%). For the low SNa (1 nmol/g body weight) injected group, 7/12 fish ovulated successfully (58%). Nine of the 12 fish in the High SNa (2.5 nmol/g body weight) injected group ovulated (75%), as well as 10/12 fish in the hCG injected group (83%) (Fig 4.3A). Injection of both doses of SNa and hCG significantly increased the number of fish who ovulated, compared to the control saline group ($p < 0.05$). There was a significant increase in the percentage of eggs ovulated in High SNa, and hCG injected groups compared to saline injected controls. The median percentages were 64%, 76%, and 79% respectively ($p > 0.05$, Fig 4.3B).

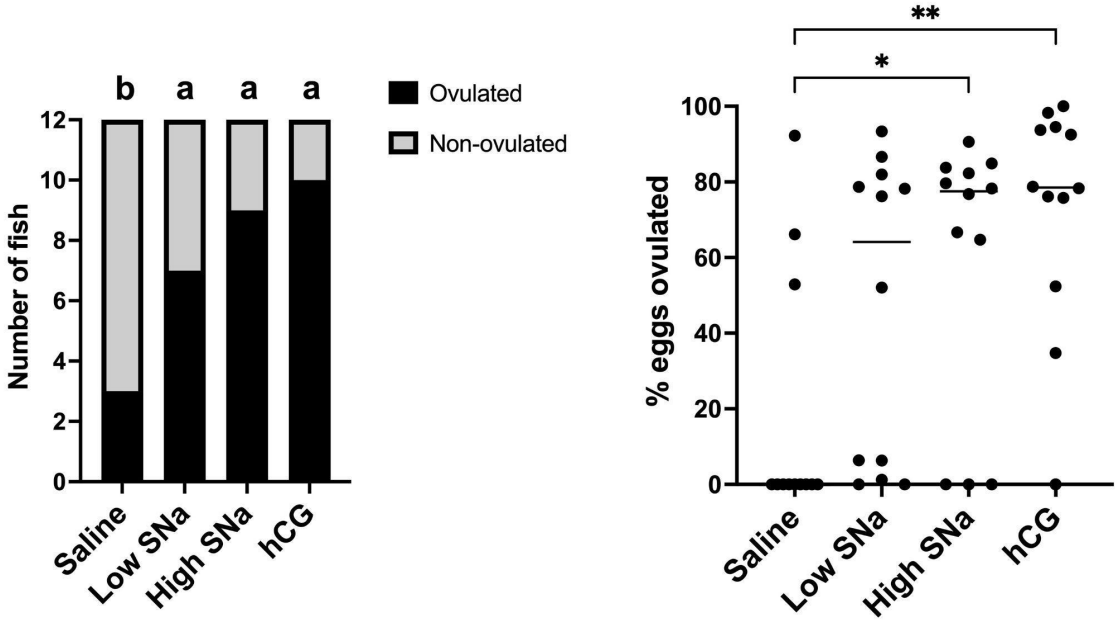

Fig 4.3 Ovulation of female zebrafish 6 hours after injection with saline, Low SNa, High SNa, or hCG. (A) The number of female fish that ovulated in each injection group were compared using Z-scores for 2 proportions using a one-tailed hypothesis. Significance is denoted by different letters ($p < 0.05$). **(B)** The percentage of total eggs that ovulated in fish injected with Saline, Low SNa, High SNa, or hCG. Results are presented as medians; Kruskal-Wallis test with Dunn's multiple comparisons test, treatment groups compared to saline control. ($p < 0.05$).

4.4 Discussion

Based on SNa neuron activation within the periovulatory period (Chapter 3), our goal in this study was to investigate the potential connection of increased SNa and Lh cell activity. Lh gonadotroph activation was observed in response to a single SNa injection of isolated, mature female zebrafish. Utilizing the validated phospho-ERK primary antibody (Chapter 2), we documented cellular activation throughout the pituitary, primarily concentrated to the PPD, as well as a dose-dependent activation of Lh cells 6 hours post i.p injection. Both the lower and higher dose of SNa elicited Lh cell activation, with the higher dose generating a significant increase compared to the saline-injected controls. These results are important, as this same i.p injection successfully induced ovulation to a level comparable to that of hCG injection, an effective Lh agonist for the induction of ovulation in zebrafish (Tang et al. 2016, Peng, 2022).

Previous work in our lab using *scg2a* frameshift mutants revealed reproductive impairments. Notably, a significant reduction in the spawning success of these fish was observed. Partial rescue by a single SNa injection was possible in these animals with a dose equivalent (1 nmol/g) to the lower dose SNa injection used in this study (Mitchell et al. 2020). Additionally, double *scg2a-/-;scg2b-/-* mutants exhibited significant reduction in ovulation compared to WT controls, thus the reduced spawning is hypothesized to be a result of failed ovulation. Indeed, pituitary *lhb* and *cga* mRNA levels are >90% lower in *scg2a-/-* females compared to WT (Mitchell et al. 2020). Reduction in spawning is significant due to the coordinated nature of egg and sperm release during fish oviposition needed for successful fertilization. The results of a previous ovulation assay in our lab (Peng, 2022) have been replicated in this study, and highlight the clear involvement of SNa in driving successful ovulation. Increasing the dosage of SNa injected increases ovulation success from 58% to 75%, which is an increase of 14 % from what Peng (2022) observed. It is important to note that the effects of the high dose of SNa on ovulation were similar to those obtained by injection of the Lh analog hCG. These results demonstrate SNa involvement in ovulation and support the proposal that SNa stimulates the Lh surge.

There was no significant difference between the number of *lhb*-expressing cells following SNa injection, but a degree of variation was observed between treatments and between individuals sampled. Injection of SNa increases *lhb* and *cga* mRNA in zebrafish within 6 hours post injection (Peng, 2022). Though other factors have been found to regulate gonadotropin subunit mRNA within a time frame relevant to the periovulatory period. GABA, a stimulatory neurotransmitter,

and other Gnrh agonists increase *lhb* subunit mRNA in goldfish with progressive ovarian maturity (Trudeau et al., 2000). Agonists for the melanocortin-4 receptor significantly increased levels of both *lhb* and *fshb* mRNA from incubated pituitary tissue of the spotted scat, *Scatophagus argus* (Jiang et al., 2017). Melanocortin-family peptides are proteolytically processed into smaller biologically active peptides from the larger POMC precursor, similar to SN processing from Scg2, and have been implicated in modulating reproduction in mammals (Ward et al., 2009; Tao, 2010) and fish (Jiang et al., 2017). Classically, Gnrh upregulates gonadotropin subunit mRNA (Stamatiades & Kaiser, 2017), with increases of *lhb* and *scg2* in the goldfish pars distalis specifically observed in response to a Gnrh agonist (Samia et al., 2004). Even within the controls, there exists basal gene expression and cellular activity, supported by the similar levels of pERK observed in all treatments, which is a challenge with using animal models. Thus, there is a complex network of factors that can and do contribute to fluctuations of *lhb* activity in the pituitary outside of SNa action, which may provide some explanation to the variation observed.

Injection of SNa stimulates Lh release and upregulates gonadotropin subunit mRNA in various models. Here we provide the first anatomical evidence of SNa activation of Lh cells in vivo. Based on SNa injections conducted by Peng (2022) with the lower SNa dose showing SNa upregulates *lhb* and *cga* mRNA 6 hours post i.p injection, we predicted that SNa activates Lh cells, and that increasing the dose may intensify this activation. By limiting our analysis to unovulated females in the saline group and only ovulated females for both SNa doses, we focussed on SNa actions on Lh cell activation. Unovulated saline injected controls do not show Lh cell activation, despite having comparable total levels of *lhb*-expressing cells and overall pERK stained cells to ovulated fish injected with low and high SNa. Compared to unovulated females, injection of SNa more than doubled the amount of Lh cell activation observed after 6 hours. High dose SNa increased this activation in ovulated females from the low dose by 2.5 times, which is 5.5 times more than that observed in the unovulated saline controls. In spotted grouper, treatment of cultured pituitary cells with SNa also generated a dose response, with *lhb* mRNA expression increasing with increasing dose (Shu et al., 2018). Increased *lhb* expression was induced in LβT2 mouse pituitary cells by incremental SNa doses, but not in a dose-dependent manner (Zhao et al., 2011). The PPD is the primary location of Lh and Fsh cells, as well as somatotrophs, the growth hormone (GH) secreting cells (Fontaine et al., 2022). Lh cell activation is concentrated to this area in fish receiving both the lower and higher SNa doses. Since SNa injections can upregulate *fshb* mRNA

after 6 hours (Shu et al., 2018), it is important to note that the other activated cells within the PPD may be Fsh-secreting gonadotrophs and needs further investigation. We provide important in vivo evidence for SNa action on gonadotrophs. Together with periovulatory activation of POA SNa neurons (Chapter 3) and activation of Lh cells following SNa injection it is proposed that SNa is a stimulatory neuropeptide in the HPG axis of zebrafish.

Chapter 5. General Discussion and Conclusion

5.1 Thesis summary

The data presented in this thesis shows SNa activity during the ovulatory cycle, highlighting the activation of neurons in the periovulatory period as well as SNa mediated activation of Lh gonadotrophs. Secretoneurin, derived from a larger precursor protein Scg2, has emerged as a candidate in teleost reproductive control. SN increases gonadotropin subunit mRNA levels (Zhao et al., 2010) and Lh secretion (Zhao et al., 2011). Injection of SNa can increase expression of neuropeptidergic and pituitary genes regulating reproduction as well as stimulate ovulation in WT female zebrafish (Peng, 2022). Moreover, the generation of double scg2a-/-, scg2b-/- TALEN frameshift mutant zebrafish revealed significant reproductive deficits, including reduction of reproduction related genes and failure to ovulate (Mitchel et al., 2020). Therefore, the Scg2a/SNa system is proposed to play an important role in regulating the teleost reproductive axis, likely promoting successful ovulation through effects on Lh. Here, we investigated the hypothesis that SNa is involved in the ovulatory process in female zebrafish because neurons are activated prior to ovulation.

The first objective of this thesis aimed to validate a commercial primary antibody for phospho-ERK to be used in subsequent studies to visualize pERK expression as a biomarker for SNa neuronal activation (Chapter 2). The mouse anti-phospho-ERK1/2 primary antibody chosen had not yet been tested in zebrafish. By testing the antibody on WT female brain and pituitary tissues, we confirmed successful immunoreaction and determined optimal dilution for strong signal visualization. The results of blocking antibody action through a custom designed phosphorylated peptide corresponding to the conserved target ERK epitope revealed this antibody generated no observable off-target binding and is therefore specific to the biologically active double phosphorylated ERK (Hussain et al., 2013; Xia et al., 1996). To verify pERK as an effective biomarker, we activated neurons by administration of S-AMPA, a glutamate agonist. S-AMPA significantly increased pERK immunoreactivity in the preoptic area and hypothalamus, while also showing increased activity in the pituitary 3 minutes post i.p injection, reinforcing these regions as important centers for neuroendocrine control. Together, the results of injecting the glutamate agonist S-AMPA verify pERK as a suitable biomarker for neuronal activation and highlight its ability to detect fast-acting changes in cell activation and thus verifying its effective use for

identifying SNa neurons activated in the periovulatory period (Chapter 3), and for pituitary cell activation following SNa injections (Chapter 4). Tracing time-dependent pERK expression with this pERK primary antibody and immunohistochemistry can be useful not only in visualization of reproduction specific neuroendocrine circuits, but also in other neuronal networks. It is a useful tool, capable of providing spatial and temporal information regarding cell activity in neural and pituitary cells.

Once establishing an optimized immunohistochemistry protocol and validation of the pERK primary antibody, we used classical breeding pairing and sampled females at key timepoints during the periovulatory period (Chapter 3). Our results revealed the first evidence of SNa-ir neurons being activated prior to ovulation in a female vertebrate. SNa-positive magnocellular neurons and some parvocellular neurons in the POA were also pERK positive, with a progressive increase in activation observed over time. These neurons also express Ist (Canosa et al., 2011; Peng, 2022), a nonapeptide important for teleost social-sexual behaviour (Mennigen et al., 2022). Based on previous evidence that SNa peptide levels in the brain are highest at 5:00h (Peng, 2022), we predicted activation would be highest at 5:00h, the time of the presumptive Lh surge. However, we observed that activation peaked at 8:30h, or just before predicted ovulation, a progressive activation of preoptic SNa neurons during and following the Lh surge. These results partially validate our original hypothesis and demonstrate successful periovulatory SNa preoptic neuron engagement.

We wanted to examine the proposed biological action of SNa on Lh gonadotrophs in the pituitary (Chapter 4). With a single injection of either saline, low dose SNa (1 nmol/g body weight), or high dose SNa (2.5 nmol/g bodyweight), we were able to simultaneously evaluate the activation of Lh cells and assess the ability of SNa to induce ovulation. Both the low and high dose of SNa induced ovulation to a level comparable to that of hCG, which was injected as a positive control. Fish that ovulated exhibited activation of Lh cells by SNa in a dose-dependent manner. Increased pERK activity in the SNa-injected fish was observed primarily in the PPD, suggesting the potential biological action of SNa on other cell types. These results provide important in vivo evidence for SNa action on gonadotrophs. Together with periovulatory activation of POA SNa neurons (Chapter 3) and activation of Lh cells following SNa injection it is proposed that SNa is a stimulatory neuropeptide in the HPG axis of zebrafish (Fig 5.1).

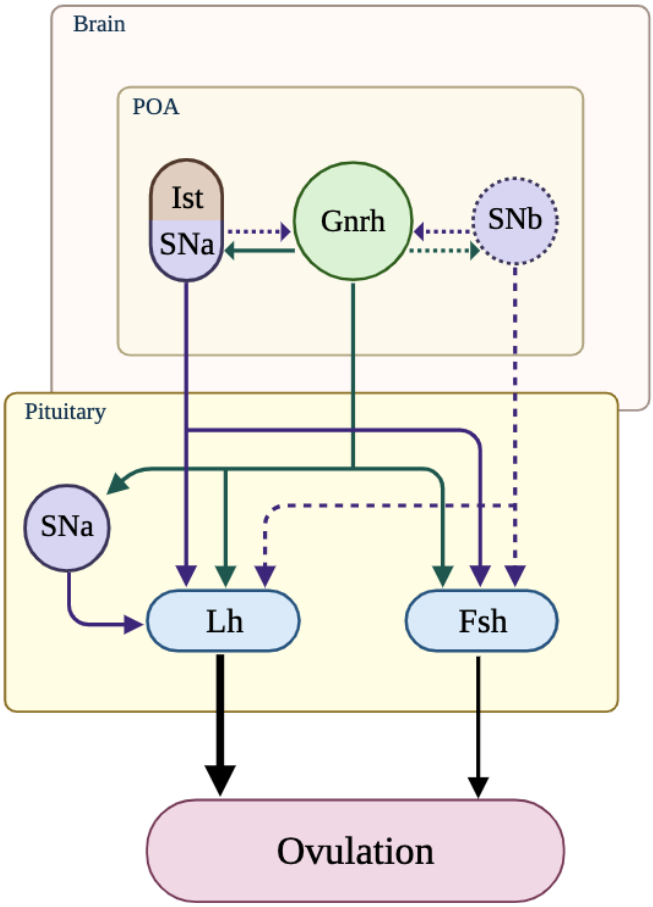

Fig 5.1 Summary of key findings and working model for SNa in zebrafish ovulation. Activation of secretoneurin A (SNa) neurons located within the preoptic area (POA) were found to progressively increase in the periovulatory period (Chapter 3). Previous documentations indicate some of these neurons are shown to be co-localized with isotocin (Ist) (Canosa et al., 2011, Peng, 2022). SNa-immunoreactive cells are also found in zebrafish pituitary. SNa i.p injection has successfully stimulated increased *lhb* and *fshb* expression (Shu et al., 2018). Injection of 1 nmol/g and 2.5 nmol/g SNa activates Lh cells (Chapter 4). These findings are key indicators of the involvement of SNa in promoting the Lh surge and ovulation. Dotted lines represent hypothesized but untested or under-studied relationships. Based on the SNa activity, SNb is hypothesized to influence gonadotrophs and the HPG axis in a similar manner and is a target of future research.

5.2 Future directions

5.2.1 Further investigation of periovulatory SNa neuron and cell activation

It is clear that preoptic SNa neurons are active in the periovulatory period, progressively between the Lh surge and presumptive ovulation. Future studies should focus on mapping more precisely when this activation increases between Lh surge and ovulation to link SNa more tightly

to Lh surge modulation. Sampling at smaller intervals, perhaps hourly, between 5:00h and 8:30h could help resolve temporal POA SNa neuron engagement before successful ovulation and elucidate the activational sequence of SNa neurons in specific subdivisions of the POA. The same strategy for investigating preoptic neuron activity should be applied to focus on other neuroendocrine regions, including olfactory bulb and hypothalamic populations of SNa, as well as SNa cells in the pituitary. Improvement and optimization of microscopy to maximize cellular resolution in these regions will be essential to adequately track pERK and SNa co-localization in these areas. There appears to be other neurons that may be activated as well so their characterization should also be considered.

5.2.2 SNa activation of Fsh cells

Using transgenic reporter lines allows researchers to visualize anatomical relationships between target regulators and effector cells, organs, and tissues. Though endogenous transgene expression can be difficult to detect in some models. We were not able to investigate the link between SNa and Fsh through i.p injections as transgene expression was weakly detected. Commercially produced primary antibodies targeting EGFP protein are well characterized and extensively validated. Visualizing *fshb*-EGFP transgene expression with an EGFP primary antibody will allow for better signal detection and make it possible to replicate the experiments done in the study to investigate isolated SNa action on Fsh cells.

5.2.3 Characterization of SNb

The work presented in this thesis is focused on SNa based on the existence of a well characterized, validated primary antibody. The existence of SNb in teleosts and the past and emerging evidence that Scg2b/SNb is important in zebrafish reproduction cannot be overlooked (Fig 5.1). Until now, there have been no SNb primary antibodies generated that detect SNb in the zebrafish brain. Our lab is in the validation stages of generating a monoclonal SNb primary antibody that is reactive in zebrafish brain and pituitary tissue. If successful, repeating the work done in this thesis with focus on SNb will be necessary to reveal the dynamic relationship between both SN paralogs and the zebrafish HPG axis.

5.3 Concluding remarks

This research contributes to basic knowledge of SN in teleost reproduction, demonstrating that SNa neuronal networks are active prior to ovulation and can activate Lh cells in the pituitary. This supports the hypothesis that the Scg2/SN system regulates teleost brain-pituitary-gonad function and contributes to the role of SN as a reproductive hormone in vertebrates.

References

Abraham, E., Palevitch, O., Gothilf, Y., & Zohar, Y. (2010). Targeted Gonadotropin-Releasing Hormone-3 Neuron Ablation in Zebrafish: Effects on Neurogenesis, Neuronal Migration, and Reproduction. *Endocrinology*, *151*(1), 332–340. https://doi.org/10.1210/EN.2009-0548

Acher, R., & Chauvet, J. (1995). The Neurohypophysial Endocrine Regulatory Cascade: Precursors, Mediators, Receptors, and Effectors. *Frontiers in Neuroendocrinology*, *16*(3), 237–289. https://doi.org/10.1006/FRNE.1995.1009

Adachi, S., Yamada, S., Takatsu, Y., Matsui, H., Kinoshita, M., Takase, K., Sugiura, H., Ohtaki, T., Matsumoto, H., Uenoyama, Y., Tsukamura, H., Inoue, K., & Maeda, K. I. (2007). Involvement of Anteroventral Periventricular Metastin/Kisspeptin Neurons in Estrogen Positive Feedback Action on Luteinizing Hormone Release in Female Rats. *Journal of Reproduction and Development*, *53*(2), 367–378. https://doi.org/10.1262/JRD.18146

Aida, K. (1988). A review of plasma hormone changes during ovulation in cyprinid fishes. *Aquaculture*, *74*(1–2), 11–21. https://doi.org/10.1016/0044-8486(88)90081-6

Aizen, J., Pang, Y., Harris, C., Converse, A., Zhu, Y., Aguirre, M. A., & Thomas, P. (2018). Roles of progesterone receptor membrane component 1 and membrane progestin receptor alpha in regulation of zebrafish oocyte maturation. *General and Comparative Endocrinology*, *263*, 51–61. https://doi.org/10.1016/J.YGCEN.2018.04.009

Almeida, O., & Oliveira, R. F. (2015). Social Status and Arginine Vasotocin Neuronal Phenotypes in a Cichlid Fish. *Brain Behavior and Evolution*, *85*(3), 203–213. https://doi.org/10.1159/000381251

Altmieme, Z., Jubouri, M., Touma, K., Coté, G., Fonseca, M., Julian, T., & Mennigen, J. A. (2019). A reproductive role for the nonapeptides vasotocin and isotocin in male zebrafish (Danio rerio) [Article]. *Comparative Biochemistry and Physiology Part - B: Biochemistry and Molecular Biology*, *238*, 110333–110333. https://doi.org/10.1016/j.cbpb.2019.110333

Amagai, T., Izumida, D., Murata, R., & Soyano, K. (2022). Male Pheromones Induce Ovulation in Female Honeycomb Groupers (Epinephelus merra): A Comprehensive Study of Spawning Aggregation Behavior and Ovarian Development [Article]. *Cells (Basel, Switzerland)*, *11*(3), 484. https://doi.org/10.3390/cells11030484

Ang, C. W., Dotman, C. H., Winkler, H., Fischer-Colbrie, R., Sonnemans, M. A. F., & Van Leeuwen, F. W. (1997). Specific expression of secretogranin II in magnocellular vasopressin neurons of the rat supraoptic and paraventricular nucleus in response to osmotic stimulation. *Brain Research*, *765*(1), 13–20. https://doi.org/10.1016/S0006-8993(97)00462-9

Bakker, J., Woodley, S. K., Kelliher, K. R., & Baum, M. J. (2002). Sexually Dimorphic Activation of Galanin Neurones in the Ferret's Dorsomedial Preoptic Area/Anterior Hypothalamus after Mating [Article]. *Journal of Neuroendocrinology*, *14*(2), 116–125. https://doi.org/10.1046/j.0007-1331.2001.00751.x

Balment, R. J., Lu, W., Weybourne, E., & Warne, J. M. (2006). Arginine vasotocin a key hormone in fish physiology and behaviour: A review with insights from mammalian models. *General and Comparative Endocrinology*, *147*(1), 9–16. https://doi.org/10.1016/J.YGCEN.2005.12.022

Baraban, S. C., Taylor, M. R., Castro, P. A., & Baier, H. (2005). Pentylenetetrazole induced changes in zebrafish behavior, neural activity and c-fos expression [Article]. *Neuroscience*, *131*(3), 759–768. https://doi.org/10.1016/j.neuroscience.2004.11.031

Blanco-Vives, B., & Sánchez-Vázquez, F. J. (2009). Synchronisation to light and feeding time of circadian rhythms of spawning and locomotor activity in zebrafish. *Physiology & Behavior*, *98*(3), 268–275. https://doi.org/10.1016/J.PHYSBEH.2009.05.015

Boczek-Leszczyk, E., Stempniak, B., & Juszczak, M. (2010). Vasopressin release from the rat hypothalamo-neurohypophysial system: effects of gonadotrophin-releasing hormone [GnRH], its analogues and melatonin. *Journal of Physiology and Pharmacology*, *61*(4), 459–466.

Bordeaux, J., Welsh, A. W., Agarwal, S., Killiam, E., Baquero, M. T., Hanna, J. A., Anagnostou, V. K., & Rimm, D. L. (2010). Antibody validation. In *BioTechniques* (Vol. 48, Issue 3, pp. 197–209). Eaton Publishing Company. https://doi.org/10.2144/000113382

Brechbuhl, H. M., Barrett, A. S., Kopin, E., Hagen, J. C., Han, A. L., Gillen, A. E., Finlay-Schultz, J., Cittelly, D. M., Owens, P., Horwitz, K. B., Sartorius, C. A., Hansen, K., & Kabos, P. (2020a). *Fibroblast subtypes define a metastatic matrisome in breast cancer*. https://doi.org/10.1172/jci.insight.130751

Brechbuhl, H. M., Barrett, A. S., Kopin, E., Hagen, J. C., Han, A. L., Gillen, A. E., Finlay-Schultz, J., Cittelly, D. M., Owens, P., Horwitz, K. B., Sartorius, C. A., Hansen, K., & Kabos, P. (2020b). Fibroblast subtypes define a metastatic matrisome in breast cancer. *JCI Insight*, *5*(4). https://doi.org/10.1172/JCI.INSIGHT.130751

Brock, O., & Bakker, J. (2013). *The Two Kisspeptin Neuronal Populations Are Differentially Organized and Activated by Estradiol in Mice*. https://doi.org/10.1210/en.2013-1120

Cancedda, L., Putignano, E., Impey, S., Maffei, L., Ratto, G. M., & Pizzorusso, T. (2003). *Behavioral/Systems/Cognitive Patterned Vision Causes CRE-Mediated Gene Expression in the Visual Cortex through PKA and ERK*.

Canosa, L. F., Lopez, G. C., Scharrig, E., Lesaux-Farmer, K., Somoza, G. M., Kah, O., & Trudeau, V. L. (2011). Forebrain mapping of secretoneurin-like immunoreactivity and its colocalization with isotocin in the preoptic nucleus and pituitary gland of goldfish. *Journal of Comparative Neurology*, *519*(18), 3748–3765. https://doi.org/10.1002/CNE.22688

Casarini, L., Santi, D., Brigante, G., & Simoni, M. (2018). Two Hormones for One Receptor: Evolution, Biochemistry, Actions, and Pathophysiology of LH and hCG. *Endocrine Reviews*, *39*(5), 549–592. https://doi.org/10.1210/ER.2018-00065

Casteel, C. O., & Singh, G. (2022). Physiology, Gonadotropin-Releasing Hormone. *StatPearls*. https://www.ncbi.nlm.nih.gov/books/NBK558992/

Chang, W. T., Liu, W., Chiu, Y. H., Chen, B. H., Chuang, S. C., Chen, Y. C., Hsu, Y. T., Lu, M. J., Chiou, S. J., Chou, C. K., & Chiu, C. C. (2017). A 4-phenoxyphenol derivative exerts inhibitory effects on human hepatocellular carcinoma cells through regulating autophagy and apoptosis accompanied by downregulating α-tubulin expression. *Molecules*, *22*(5). https://doi.org/10.3390/molecules22050854

Chen, R.-H., Sarnecki, C., & Blenis, J. (1992). Nuclear localization and regulation of erk- and rsk-encoded protein kinases. *Molecular and Cellular Biology*, *12*(3), 915–927. https://doi.org/10.1128/MCB.12.3.915

Christian, C. A., Mobley, J. L., & Moenter, S. M. (2005). *Diurnal and estradiol-dependent changes in gonadotropin-releasing hormone neuron firing activity*. www.pnas.orgcgidoi10.1073pnas.0504270102

Chuderland, D., & Seger, R. (2005). Protein-protein interactions in the regulation of the extracellular signal-regulated kinase. *Molecular Biotechnology*, *29*(1), 57–74. https://doi.org/10.1385/MB:29:1:57

Dai, Y., Iwata, K., Fukuoka, T., Kondo, E., Tokunaga, A., Yamanaka, H., Tachibana, T., Liu, Y., & Noguchi, K. (2002). *Phosphorylation of Extracellular Signal-Regulated Kinase in Primary Afferent Neurons by Noxious Stimuli and Its Involvement in Peripheral Sensitization*.

De Tassigny, X. D. A., Fagg, L. A., Carlton, M. B. L., & Colledge, W. H. (2008). Kisspeptin Can Stimulate Gonadotropin-Releasing Hormone (GnRH) Release by a Direct Action at GnRH Nerve Terminals. *Endocrinology*, *149*(8), 3926–3932. https://doi.org/10.1210/EN.2007-1487

Demski, L. S., & Knigge, K. M. (1971). The telencephalon and hypothalamus of the bluegill (Lepomis macrochirus): Evoked feeding, aggressive and reproductive behavior with representative frontal sections. *Journal of Comparative Neurology*, *143*(1), 1–16. https://doi.org/10.1002/cne.901430102

Ducret, E., Anderson, G. M., & Herbison, A. E. (2009). RFamide-Related Peptide-3, a Mammalian Gonadotropin-Inhibitory Hormone Ortholog, Regulates Gonadotropin-Releasing Hormone Neuron Firing in the Mouse. *Endocrinology*, *150*(6), 2799–2804. https://doi.org/10.1210/EN.2008-1623

Edwards, J. G., & Michel, W. C. (2002). Odor-stimulated glutamatergic neurotransmission in the zebrafish olfactory bulb. *Journal of Comparative Neurology*, *454*(3), 294–309. https://doi.org/10.1002/cne.10445

Espey, L. L. (1980). Ovulation as an Inflammatory Reaction—A Hypothesis. *Biology of Reproduction*, *22*(1), 73–106. https://doi.org/10.1095/BIOLREPROD22.1.73

Espey, L. L., & Richards, J. S. (2006). *Ovulation*.

Espigares, F., Rocha, A., Gómez, A., Carrillo, M., & Zanuy, S. (2017). Photoperiod modulates the reproductive axis of European sea bass through regulation of kiss1 and gnrh2 neuronal expression. *General and Comparative Endocrinology*, *240*, 35–45. https://doi.org/10.1016/J.YGCEN.2016.09.007

Fontaine, R., Royan, M. R., Henkel, C., Hodne, K., Ager-Wick, E., & Weltzien, F.-A. (2022). Pituitary multi-hormone cells in mammals and fish: history, origin, and roles. *Frontiers in Neuroendocrinology*, *67*, 101018. https://doi.org/10.1016/j.yfrne.2022.101018

Foran, C. M., & Bass, A. H. (1998). *Preoptic AVT Immunoreactive Neurons of a Teleost Fish with Alternative Reproductive Tactics*.

Fuller, C. L., Yettaw, H. K., & Byrd, C. A. (2006). Mitral cells in the olfactory bulb of adult zebrafish (Danio rerio): Morphology and distribution. *Journal of Comparative Neurology*, *499*(2), 218–230. https://doi.org/10.1002/CNE.21091

Gao, Y.-J., & Ji, R.-R. (2009). c-Fos or pERK, Which is a Better Marker for Neuronal Activation and Central Sensitization After Noxious Stimulation and Tissue Injury? *The Open Pain Journal*, *2*(1), 11–17. https://doi.org/10.2174/1876386300902010011

Geuna, S. (2000). Commentary Appreciating the Difference Between Design-Based and Model-Based Sampling Strategies in Quantitative Morphology of the Nervous System. *J. Comp. Neurol*, *427*, 333–339. https://doi.org/10.1002/1096-9861

Giannecchini, L. G., Massago, H., & Fernandes, J. B. K. (2012). Effects of photoperiod on reproduction of Siamese fighting fish Betta splendens. *Revista Brasileira de Zootecnia*, *41*(4), 821–826. https://doi.org/10.1590/S1516-35982012000400001

Goetz, F. W., & Garczynski, M. (1997). *The ovarian regulation of ovulation in teleost fish*.

Golan, M., Biran, J., Levavi-Sivan, B., Conn, P. M., & Childs, G. V. (2014). *A novel model for development, organization, and function of gonadotropes in fish pituitary*. https://doi.org/10.3389/fendo.2014.00182

Goodman, R. L., Herbison, A. E., Lehman, M. N., & Navarro, V. M. (2022). Neuroendocrine control of gonadotropin-releasing hormone: Pulsatile and surge modes of secretion. *Journal of Neuroendocrinology*, *34*(5), e13094. https://doi.org/10.1111/jne.13094

Goodson, J. L. (2005). The vertebrate social behavior network: Evolutionary themes and variations. *Hormones and Behavior*, *48*(1 SPEC. ISS.), 11–22. https://doi.org/10.1016/j.yhbeh.2005.02.003

Goodson, J. L. (2008). Nonapeptides and the evolutionary patterning of sociality. *Progress in Brain Research*, *170*, 3–15. https://doi.org/10.1016/S0079-6123(08)00401-9

Goodson, J. L., & Bass, A. H. (2001). Social behavior functions and related anatomical characteristics of vasotocin/vasopressin systems in vertebrates. *Brain Research Reviews*, *35*(3), 246–265. https://doi.org/10.1016/S0165-0173(01)00043-1

Goodson, J. L., Kelly, A. M., & Kingsbury, M. A. (2012). Evolving nonapeptide mechanisms of gregariousness and social diversity in birds. *Hormones and Behavior*, *61*(3), 239–250. https://doi.org/10.1016/J.YHBEH.2012.01.005

Hart, B. L., Haugen, C. M., & Peterson, D. M. (1973). EFFECTS OF MEDIAL PREOPTIC-ANTERIOR HYPOTHALAMIC LESIONS ON MATING BEHAVIOR OF MALE CATS. *Brain Research*, *54*, 177–191.

Harter, C. J. L., Kavanagh, G. S., & Smith, J. T. (2018). The role of kisspeptin neurons in reproduction and metabolism. *Journal of Endocrinology*, *238*(3), R173–R183. https://doi.org/10.1530/JOE-18-0108

Hellier, V., Brock, O., Candlish, M., Desroziers, E., Aoki, M., Mayer, C., Piet, R., Herbison, A., Colledge, W. H., Prévot, V., Boehm, U., & Bakker, J. (2018). Female sexual behavior in mice is controlled by kisspeptin neurons. *Nature Communications 2018 9:1*, *9*(1), 1–12. https://doi.org/10.1038/s41467-017-02797-2

Hermanowicz, J. M., Pawlak, K., Sieklucka, B., Czarnomysy, R., Kwiatkowska, I., Kazberuk, A., Surazynski, A., Mojzych, M., & Pawlak, D. (2021). MM-129 as a Novel Inhibitor Targeting PI3K/AKT/mTOR and PD-L1 in Colorectal Cancer. *Cancers*, *13*(13). https://doi.org/10.3390/CANCERS13133203

Hoflehner, J., Eder, U., Laslop, A., Seidah, N. G., Fischer-Colbrie, R., & Winkler, H. (1995). Processing of secretogranin II by prohormone convertases: Importance ofPC1 in generation of secretoneurin. *FEBS Letters*, *360*(3), 294–298. https://doi.org/10.1016/0014-5793(95)00127-U

Howat, W. J., Lewis, A., Jones, P., Kampf, C., Pontén, F., van der Loos, C. M., Gray, N., Womack, C., & Warford, A. (2014). Antibody validation of immunohistochemistry for biomarker discovery: Recommendations of a consortium of academic and pharmaceutical based histopathology researchers. *Methods*, *70*(1), 34–38. https://doi.org/10.1016/j.ymeth.2014.01.018

Hussain, A., Saraiva, L. R., Ferrero, D. M., Ahuja, G., Krishna, V. S., Liberles, S. D., & Korsching, S. I. (2013). High-affinity olfactory receptor for the death-associated odor cadaverine. *Proceedings of the National Academy of Sciences of the United States of America*, *110*(48), 19579–19584. https://doi.org/10.1073/pnas.1318596110

Jiang, D. N., Li, J. T., Tao, Y. X., Chen, H. P., Deng, S. P., Zhu, C. H., & Li, G. L. (2017). Effects of melanocortin-4 receptor agonists and antagonists on expression of genes related

to reproduction in spotted scat, Scatophagus argus. *Journal of Comparative Physiology B: Biochemical, Systemic, and Environmental Physiology*, *187*(4), 603–612. https://doi.org/10.1007/S00360-017-1062-0/FIGURES/6

Johnston, C. A., Lopez, F., Samson, W. K., & Negro-Vilar, A. (1990). Physiologically important role for central oxytocin in the preovulatory release of luteinizing hormone. *Neuroscience Letters*, *120*(2), 256–258. https://doi.org/10.1016/0304-3940(90)90053-C

Juszczak, M., & Boczek-Leszczyk, E. (2010). Hypothalamic gonadotropin-releasing hormone receptor activation stimulates oxytocin release from the rat hypothalamo-neurohypophysial system while melatonin inhibits this process. *Brain Research Bulletin*, *81*(1), 185–190. https://doi.org/10.1016/j.brainresbull.2009.10.012

Kanda, S. (2019). Evolution of the regulatory mechanisms for the hypothalamic-pituitary-gonadal axis in vertebrates–hypothesis from a comparative view. *General and Comparative Endocrinology*, *284*. https://doi.org/10.1016/J.YGCEN.2018.11.014

Kato, S., Endoh, H., Masuhiro, Y., Kitamoto, T., Uchiyama, S., Sasaki, H., Masushige, S., Gotoh, Y., Nishida, E., Kawashima, H., Metzger, D., & Chambon, P. (1995). Activation of the Estrogen Receptor Through Phosphorylation by Mitogen-Activated Protein Kinase [Article]. *Science (American Association for the Advancement of Science)*, *270*(5241), 1491–1494. https://doi.org/10.1126/science.270.5241.1491

Kermen, F., Franco, L. M., Wyatt, C., Yaksi, E., Brunjes, P., Jesuthasan, S., & Nus, D. /. (2013). *"fncir-07-00062"-2013/4/9-21:55-page 1-#1 Neural circuits mediating olfactory-driven behavior in fish*. https://doi.org/10.3389/fncir.2013.00062

Kirchmair, R., Hogue-Angeletti, R., Gutierrez, J., Fischer-Colbrie, R., & Winkler, H. (1993). Secretoneurin--a neuropeptide generated in brain, adrenal medulla and other endocrine tissues by proteolytic processing of secretogranin II (chromogranin C). *Neuroscience*, *53*(2), 359–365. https://doi.org/10.1016/0306-4522(93)90200-Y

Kumar, T. R. (2005). What have we learned about gonadotropin function from gonadotropin subunit and receptor knockout mice? *Reproduction*, *130*(3), 293–302. https://doi.org/10.1530/REP.1.00660

Luong, K., Bernardo, M. F., Lindstrom, M., Alluri, R. K., & Rose, G. J. (2023). Brain regions controlling courtship behavior in the bluehead wrasse. *Current Biology*, *33*(22), 4937-4949.e3. https://doi.org/10.1016/j.cub.2023.10.003

Ma, X., Dong, Y., Matzuk, M. M., & Kumar, T. R. (2004). Targeted disruption of luteinizing hormone β-subunit leads to hypogonadism, defects in gonadal steroidogenesis, and infertility. *Proceedings of the National Academy of Sciences of the United States of America*, *101*(49), 17294–17299. https://doi.org/10.1073/PNAS.0404743101/SUPPL_FILE/04743FIG8.PDF

Maik-Rachline, G., Hacohen-Lev-Ran, A., & Seger, R. (2019). Nuclear ERK: Mechanism of Translocation, Substrates, and Role in Cancer. *International Journal of Molecular Sciences*, *20*(5). https://doi.org/10.3390/IJMS20051194

Markham, M. R., Aguilar-Roblero, R., Ralph, M., Silva, A., Pouso, P., Cabana, Á., & Goodson, J. L. (2019a). *Preoptic Area Activation and Vasotocin Involvement in the Reproductive Behavior of a Weakly Pulse-Type Electric Fish, Brachyhypopomus gauderio*. https://doi.org/10.3389/fnint.2019.00037

Markham, M. R., Aguilar-Roblero, R., Ralph, M., Silva, A., Pouso, P., Cabana, Á., & Goodson, J. L. (2019b). *Preoptic Area Activation and Vasotocin Involvement in the Reproductive*

Behavior of a Weakly Pulse-Type Electric Fish, Brachyhypopomus gauderio. https://doi.org/10.3389/fnint.2019.00037

Marvel, M., Spicer, O. S., Wong, T. T., Zmora, N., & Zohar, Y. (2018). Knockout of the Gnrh genes in zebrafish: effects on reproduction and potential compensation by reproductive and feeding-related neuropeptides. *Biology of Reproduction*, *99*(3), 565–577. https://doi.org/10.1093/BIOLRE/IOY078

Melli, M. S., Tagavi, S., Alizadeh, M., Ghojazadeh, M., & Sheshvan, M. K. (2007). Comparison the effect of oxytocin and human chorionic gonadotropin on ovulation. *Journal of Medical Sciences*, *7*(7), 1126–1134. https://doi.org/10.3923/JMS.2007.1126.1134

Mennigen, J. A., Ramachandran, D., Shaw, K., Chaube, R., Joy, K. P., & Trudeau, V. L. (2022a). Reproductive roles of the vasopressin/oxytocin neuropeptide family in teleost fishes. *Frontiers in Endocrinology*, *13*. https://doi.org/10.3389/FENDO.2022.1005863

Mennigen, J. A., Ramachandran, D., Shaw, K., Chaube, R., Joy, K. P., & Trudeau, V. L. (2022b). Reproductive roles of the vasopressin/oxytocin neuropeptide family in teleost fishes. In *Frontiers in Endocrinology* (Vol. 13). Frontiers Media S.A. https://doi.org/10.3389/fendo.2022.1005863

Migaud, H., Davie, A., & Taylor, J. F. (2010). Current knowledge on the photoneuroendocrine regulation of reproduction in temperate fish species [Article]. *Journal of Fish Biology*, *76*(1), 27–68. https://doi.org/10.1111/j.1095-8649.2009.02500.x

Mitchell, K. (2018). Characterization and Role of Secretogranin-II/Secretoneurin in Zebrafish Reproduction. [Doctoral Dissertation, Université d'Ottawa / University of Ottawa]. E-theses uOttawa.

Mitchell, K., Mikwar, M., Da Fonte, D., Lu, C., Tao, B., Peng, D., Udeesha Erandani, W. K. C., Hu, W., & Trudeau, V. L. (2020). *Secretoneurin is a secretogranin-2 derived hormonal peptide in vertebrate neuroendocrine systems*. https://doi.org/10.1016/j.ygcen.2020.113588

Mitchell, K., Zhang, W. S., Lu, C., Tao, B., Chen, L., Hu, W., & Trudeau, V. L. (2020). Targeted mutation of secretogranin-2 disrupts sexual behavior and reproduction in zebrafish. *Proceedings of the National Academy of Sciences of the United States of America*, *117*(23), 12772–12783. https://doi.org/10.1073/PNAS.2002004117/SUPPL_FILE/PNAS.2002004117.SM04.MP4

Nagahama, Y., & Yamashita, M. (2008). Regulation of oocyte maturation in fish. *Development, Growth & Differentiation*, *50*(SUPPL. 1), S195–S219. https://doi.org/10.1111/J.1440-169X.2008.01019.X

Nicol, L., McNeilly, J. R., Stridsberg, M., & McNeilly, A. S. (2004). Differential secretion of gonadotrophins: investigation of the role of secretogranin II and chromogranin A in the release of LH and FSH in LbetaT2 cells. *Journal of Molecular Endocrinology*, *32*(2), 467–480. https://doi.org/10.1677/JME.0.0320467

Norris, D. O., & Carr, J. A. (2021). *Vertebrate endocrinology.* (Sixth). Academic Press.

O'Hurley, G., Sj, E., Ostedt, €, Rahman, A., Li, B., Kampf, C., Pont En, F., Gallagher, W. M., & Lindskog, C. (2014). *Review Garbage in, garbage out: A critical evaluation of strategies used for validation of immunohistochemical biomarkers*. https://doi.org/10.1016/j.molonc.2014.03.008

Oka, Y. (2023). Neuroendocrine regulation of reproduction by GnRH neurons: multidisciplinary studies using a small fish brain model. *Endocrine Journal*, *70*(4), 343–358. https://doi.org/10.1507/ENDOCRJ.EJ22-0669

Okuyama, T., Suehiro, Y., Imada, H., Shimada, A., Naruse, K., Takeda, H., Kubo, T., & Takeuchi, H. (2011). Induction of c-fos transcription in the medaka brain (Oryzias latipes) in response to mating stimuli [Article]. *Biochemical and Biophysical Research Communications*, *404*(1), 453–457. https://doi.org/10.1016/j.bbrc.2010.11.143

Peng, Di. (2022). Characterization and Role of Secretoneurin in Ovulatory Cycle of Zebrafish. [Doctoral Dissertation, Université d'Ottawa / University of Ottawa]. E-theses uOttawa.

Pestronk, A., Sinha, N., Alhumayyd, Z., Ly, C., Schmidt, R., & Bucelli, R. (2019). Immune myopathy with large histiocyte-related myofiber necrosis. *Neurology*, *92*(15), e1763–e1772. https://doi.org/10.1212/WNL.0000000000007260

Popesku, J. T., Mennigen, J. A., Chang, J. P., & Trudeau, V. L. (2011). Dopamine D1 Receptor Blockage Potentiates AMPA-Stimulated Luteinising Hormone Release in the Goldfish [Article]. *Journal of Neuroendocrinology*, *23*(4), 302–309. https://doi.org/10.1111/j.1365-2826.2011.02114.x

Pouso, P., Cabana, Á., Goodson, J. L., & Silva, A. (2019). Preoptic Area Activation and Vasotocin Involvement in the Reproductive Behavior of a Weakly Pulse-Type Electric Fish, Brachyhypopomus gauderio. *Frontiers in Integrative Neuroscience*, *13*, 468726. https://doi.org/10.3389/FNINT.2019.00037/BIBTEX

Randlett, O., Wee, C. L., Naumann, E. A., Nnaemeka, O., Schoppik, D., Fitzgerald, J. E., Portugues, R., Lacoste, A. M. B., Riegler, C., Engert, F., & Schier, A. F. (2015). Whole-brain activity mapping onto a zebrafish brain atlas. *Nature Methods*, *12*(11), 1039–1046. https://doi.org/10.1038/nmeth.3581

Ru-Rong Ji, Hiroshi Baba, Gary J. Brenner, & Clifford J. Woolf. (1999). Nociceptive-specific activation ofERK in spinal neurons contributesto pain hypersensitivity. *Nature Neuroscience*.

Samia, M., Larivière, K. E., Rochon, M. H., Hibbert, B. M., Basak, A., & Trudeau, V. L. (2004). Seasonal cyclicity of secretogranin-II expression and its modulation by sex steroids and GnRH in the female goldWsh pituitary. *General and Comparative Endocrinology*, *139*, 198–205. https://doi.org/10.1016/j.ygcen.2004.09.004

Scaia, M. F., Akinrinade, I., Petri, G., & Oliveira, R. F. (2022). Sex Differences in Aggression Are Paralleled by Differential Activation of the Brain Social Decision-Making Network in Zebrafish. *Frontiers in Behavioral Neuroscience*, *16*. https://doi.org/10.3389/fnbeh.2022.784835

Schnaber, E., Mains, R. E., & Farquhar, M. G. (1989). Proteolytic Processing of Pro-ACTH/Endorphin Begins in the Golgi Complex of Pituitary Corticotropes and AtT-20 Cells. *Molecular Endocrinology*, *3*(8), 1223–1235. https://doi.org/10.1210/MEND-3-8-1223

Sellix, M. T., & Menaker, M. (2010). Circadian Clocks in the Ovary. *Trends in Endocrinology and Metabolism: TEM*, *21*(10), 628. https://doi.org/10.1016/J.TEM.2010.06.002

Shu, H., Yang, L., Zhang, Y., Liu, X., Lin, H., & Li, S. (2018). Identification and functional characterization of two Secretogranin II genes in orange-spotted grouper (Epinephelus coioides). *General and Comparative Endocrinology*, *261*, 115–126. https://doi.org/10.1016/j.ygcen.2018.02.010

So, W. K., Kwok, H. F., & Ge, W. (2005). Zebrafish Gonadotropins and Their Receptors: II. Cloning and Characterization of Zebrafish Follicle-Stimulating Hormone and Luteinizing Hormone Subunits—Their Spatial-Temporal Expression Patterns and Receptor Specificity. *Biology of Reproduction*, *72*(6), 1382–1396. https://doi.org/10.1095/BIOLREPROD.104.038216

Søland, T. M., Husvik, C., Koppang, H. S., Boysen, M., Sandvik, L., Clausen, O. P. F., Christoffersen, T., & Bryne, M. (2008). A study of phosphorylated ERK1/2 and COX-2 in early stage (T1-T2) oral squamous cell carcinomas. *Journal of Oral Pathology & Medicine : Official Publication of the International Association of Oral Pathologists and the American Academy of Oral Pathology*, *37*(9), 535–542. https://doi.org/10.1111/J.1600-0714.2008.00656.X

Spicer, O. S., Wong, T. T., Zmora, N., & Zohar, Y. (2016). Targeted Mutagenesis of the Hypophysiotropic Gnrh3 in Zebrafish (Danio rerio) Reveals No Effects on Reproductive Performance. *PLOS ONE*, *11*(6), e0158141. https://doi.org/10.1371/JOURNAL.PONE.0158141

Stacey, N. E., & Kyle, A. L. (1983). Effects of Olfactory Tract Lesions on Sexual and Feeding Behavior in the Goldfish. In *Physiology & Behavior* (Vol. 30). Pergamon Press Ltd.

Stacey, N. E., & Pandey, S. (1975). Effects of indomethacin and prostaglandins on ovulation of goldfish [Article]. *Prostaglandins*, *9*(4), 597–607. https://doi.org/10.1016/0090-6980(75)90065-9

Stamatiades, G. A., & Kaiser, U. B. (2017). *Gonadotropin regulation by pulsatile GnRH: Signaling and gene expression*. https://doi.org/10.1016/j.mce.2017.10.015

Su, B., Shi, D., Jiao Tong University, S., Fang Yuan, C., Qin, Z., Qin, L., Yan, J., Jia, J., Sun, Y., Wang, H., Wang, W., Lu, J., Zhang, J., Luo, X., Luan, L., & Wang, K. (2022). OPEN ACCESS EDITED BY Glutamatergic and GABAergic neurons in the preoptic area of the hypothalamus play key roles in menopausal hot flashes. *TYPE Original Research PUBLISHED*, *14*. https://doi.org/10.3389/fnagi.2022.993955

Takahashi, A., Kanda, S., Abe, T., & Oka, Y. (2016). Evolution of the Hypothalamic-Pituitary-Gonadal Axis Regulation in Vertebrates Revealed by Knockout Medaka. *Endocrinology*, *157*(10), 3994–4002. https://doi.org/10.1210/EN.2016-1356

Tang, H., Liu, Y., Li, J., Yin, Y., Li, G., Chen, Y., Li, S., Zhang, Y., Lin, H., Liu, X., & Cheng, C. H. K. (2016). Gene knockout of nuclear progesterone receptor provides insights into the regulation of ovulation by LH signaling in zebrafish OPEN. *Nature Publishing Group*. https://doi.org/10.1038/srep28545

Tang, H., Liu, Y., Luo, D., Ogawa, S., Yin, Y., Li, S., Zhang, Y., Hu, W., Parhar, I. S., Lin, H., Liu, X., & Cheng, C. H. K. (2015). *The kiss/kissr Systems Are Dispensable for Zebrafish Reproduction: Evidence From Gene Knockout Studies*. https://doi.org/10.1210/en.2014-1204

Tao, B., Hu, H., Mitchell, K., Chen, J., Jia, H., Zhu, Z., Trudeau, V. L., & Hu, W. (2018). Secretogranin-II plays a critical role in zebrafish neurovascular modeling. *Journal of Molecular Cell Biology*, *10*(5), 388–401. https://doi.org/10.1093/jmcb/mjy027

Tao, Y. X. (2010). The melanocortin-4 receptor: physiology, pharmacology, and pathophysiology. *Endocrine Reviews*, *31*(4), 506–543. https://doi.org/10.1210/ER.2009-0037

Taziaux, M., & Bakker, J. (2015). Absence of female-typical pheromone-induced hypothalamic neural responses and kisspeptin neuronal activity in α-fetoprotein knockout female mice. *Endocrinology*, *156*(7), 2595–2607. https://doi.org/10.1210/en.2015-1062

Troger, J., Theurl, M., Kirchmair, R., Pasqua, T., Tota, B., Angelone, T., Cerra, M. C., Nowosielski, Y., Mätzler, R., Troger, J., Gayen, J. R., Trudeau, V., Corti, A., & Helle, K. B. (2017). Granin-derived peptides. *Progress in Neurobiology*, *154*, 37–61. https://doi.org/10.1016/J.PNEUROBIO.2017.04.003

Trudeau, V. L. (2021). *Neuroendocrine Control of Reproduction in Teleost Fish: Concepts and Controversies*. https://doi.org/10.1146/annurev-animal-020420

Trudeau, V. L., Martyniuk, C. J., Zhao, E., Hu, H., Volkoff, H., Decatur, W. A., & Basak, A. (2012). Is secretoneurin a new hormone? In *General and Comparative Endocrinology* (Vol. 175, Issue 1, pp. 10–18). Academic Press Inc. https://doi.org/10.1016/j.ygcen.2011.10.008

Trudeau, V. L., Shaw, K., Spadacini, V., & Hu, W. (2023). *Chapter 2 Reproductive neuroendocrinology in teleost fishes*. Preprint.

Trudeau, V. L., & Somoza, G. M. (2020). Multimodal hypothalamo-hypophysial communication in the vertebrates. *General and Comparative Endocrinology*, *293*, 113475. https://doi.org/10.1016/J.YGCEN.2020.113475

Trudeau, V. L., Spanswick, D., Fraser, E. J., Lariviere, K., Crump, D., Chiu, S., MacMillan, M., & Schulz, R. W. (2000). The role of amino acid neurotransmitters in the regulation of pituitary gonadotropin release in fish. *Https://Doi-Org.Proxy.Bib.Uottawa.ca/10.1139/O99-075*, *78*(3), 241–259. https://doi.org/10.1139/O99-075

Trudeau, V. L. (1997). Neuroendocrine regulation of gonadotrophin II release and gonadal growth in the goldfish, Carassius auratus. *Reviews of Reproduction*, *2*(1), 55–68. https://doi.org/10.1530/ROR.0.0020055

Tsafriri', A., & Reich2, R. (1999). Molecular aspects of mammalian ovulation. In *Exp Clin Endocrinol Diabetes* (Vol. 107).

Tse, A. C. K., & Ge, W. (2010). Spatial localization of EGF family ligands and receptors in the zebrafish ovarian follicle and their expression profiles during folliculogenesis. *General and Comparative Endocrinology*, *167*(3), 397–407. https://doi.org/10.1016/J.YGCEN.2009.09.012

Urano, A., & Ando, H. (2011). Diversity of the hypothalamo-neurohypophysial system and its hormonal genes. *General and Comparative Endocrinology*, *170*(1), 41–56. https://doi.org/10.1016/J.YGCEN.2010.09.016

Vaudry, H., & Conlon, J. M. (1991). Identification of a peptide arising from the specific post-translation processing of secretogranin II. *FEBS Letters*, *284*(1), 31–33. https://doi.org/10.1016/0014-5793(91)80754-Q

Wang, J. Q., Fibuch, E. E., & Mao, L. (2007). Regulation of mitogen-activated protein kinases by glutamate receptors. *Journal of Neurochemistry*, *100*(1), 1–11. https://doi.org/10.1111/J.1471-4159.2006.04208.X

Ward, D. R., Dear, F. M., Ward, I. A., Anderson, S. I., Spergel, D. J., Smith, P. A., & Ebling, F. J. P. (2009). Innervation of Gonadotropin-Releasing Hormone Neurons by Peptidergic Neurons Conveying Circadian or Energy Balance Information in the Mouse. *PLOS ONE*, *4*(4), e5322. https://doi.org/10.1371/JOURNAL.PONE.0005322

Wei, N., Kakar, S. S., & Neill, J. D. (1995). Measurement of secretogranin II release from individual adenohypophysial gonadotropes [Article]. *American Journal of Physiology - Endocrinology And Metabolism*, *268*(1), 145–152. https://doi.org/10.1152/ajpendo.1995.268.1.e145

Wortzel, I., & Seger, R. (2011). The ERK cascade: Distinct functions within various subcellular organelles. In *Genes and Cancer* (Vol. 2, Issue 3, pp. 195–209). SAGE Publications Inc. https://doi.org/10.1177/1947601911407328

Wullimann, M. F., Rupp, B., & Reichert, H. (1996). *Neuroanatomy of the zebrafish brain : a topological atlas*. Birkhäuser Verlag.

Xia, Z., Dudek, H., Miranti, C. K., & Greenberg, M. E. (1996). Calcium influx via the NMDA receptor induces immediate early gene transcription by a MAP kinase/ERK-dependent mechanism. *The Journal of Neuroscience : The Official Journal of the Society for Neuroscience*, *16*(17), 5425–5436. https://doi.org/10.1523/JNEUROSCI.16-17-05425.1996

Xie, Y., & Dorsky, R. I. (2017). Development of the hypothalamus: conservation, modification and innovation. *Development (Cambridge, England)*, *144*(9), 1588–1599. https://doi.org/10.1242/DEV.139055

Yang, L. C., Zhang, Q. G., Zhou, C. F., Yang, F., Zhang, Y. D., Wang, R. M., & Brann, D. W. (2010). Extranuclear estrogen receptors mediate the neuroprotective effects of estrogen in the rat hippocampus. *PloS One*, *5*(5). https://doi.org/10.1371/JOURNAL.PONE.0009851

Yokoi, S., Naruse, K., Kamei, Y., Ansai, S., Kinoshita, M., Mito, M., Iwasaki, S., Inoue, S., Okuyama, T., Nakagawa, S., Young, L. J., & Takeuchi, H. (2020). Sexually dimorphic role of oxytocin in medaka mate choice. *Proceedings of the National Academy of Sciences of the United States of America*, *117*(9), 4802–4808. https://doi.org/10.1073/PNAS.1921446117/SUPPL_FILE/PNAS.1921446117.SM02.MP4

Zhang, W., Scerbo, P., Delagrange, M., Candat, V., Mayr, V., Vriz, S., Distel, M., Ducos, B., & Bensimon, D. (2022). Fgf8 dynamics and critical slowing down may account for the temperature independence of somitogenesis. *Communications Biology*, *5*(1). https://doi.org/10.1038/S42003-022-03053-0

Zhang, Z., Zhu, B., & Ge, W. (2015). Genetic Analysis of Zebrafish Gonadotropin (FSH and LH) Functions by TALEN-Mediated Gene Disruption. *Molecular Endocrinology*, *29*(1), 76–98. https://doi.org/10.1210/ME.2014-1256

Zhao, E., Basak, A., Crump, K., & Trudeau, V. L. (2006). Proteolytic processing and diVerential distribution of secretogranin-II in goldWsh. *General and Comparative Endocrinology*, *146*, 100–107. https://doi.org/10.1016/j.ygcen.2005.10.007

Zhao, E., Basak, A., & Trudeau, V. L. (2006). Secretoneurin stimulates goldfish pituitary luteinizing hormone production [Article]. *Neuropeptides (Edinburgh)*, *40*(4), 275–282. https://doi.org/10.1016/j.npep.2006.05.002

Zhao, E., Hu, H., & Trudeau, V. L. (2009). *Secretoneurin as a hormone regulator in the pituitary*. https://doi.org/10.1016/j.regpep.2009.11.019

Zhao, E., Mcneilly, J. R., McNeilly, A. S., Fischer-Colbrie, R., Basak, A., Seong, J. Y., & Trudeau, V. L. (2011). Secretoneurin stimulates the production and release of luteinizing hormone in mouse LβT2 gonadotropin cells. *American Journal of Physiology - Endocrinology and Metabolism*, *301*(2), E288. https://doi.org/10.1152/AJPENDO.00070.2011

Zhao, Y., Lin, M. C. A., Mock, A., Yang, M., & Wayne, N. L. (2014). Kisspeptins Modulate the Biology of Multiple Populations of Gonadotropin-Releasing Hormone Neurons during Embryogenesis and Adulthood in Zebrafish (Danio rerio). *PLOS ONE*, *9*(8), e104330. https://doi.org/10.1371/JOURNAL.PONE.0104330

Zhao, Y., Lin, M.-C. A., Farajzadeh, M., & Wayne, N. L. (2013). Early Development of the Gonadotropin-Releasing Hormone Neuronal Network in Transgenic Zebrafish. *Frontiers in Endocrinology*, *4*, 107. https://doi.org/10.3389/FENDO.2013.00107

Zohar, Y., Zmora, N., Trudeau, V. L., Muñoz-Cueto, J. A., & Golan, M. (2021). A half century of fish gonadotropin-releasing hormones: Breaking paradigms. *Journal of Neuroendocrinology*, *34*(5), e13069. https://doi.org/10.1111/JNE.13069

Appendix 1

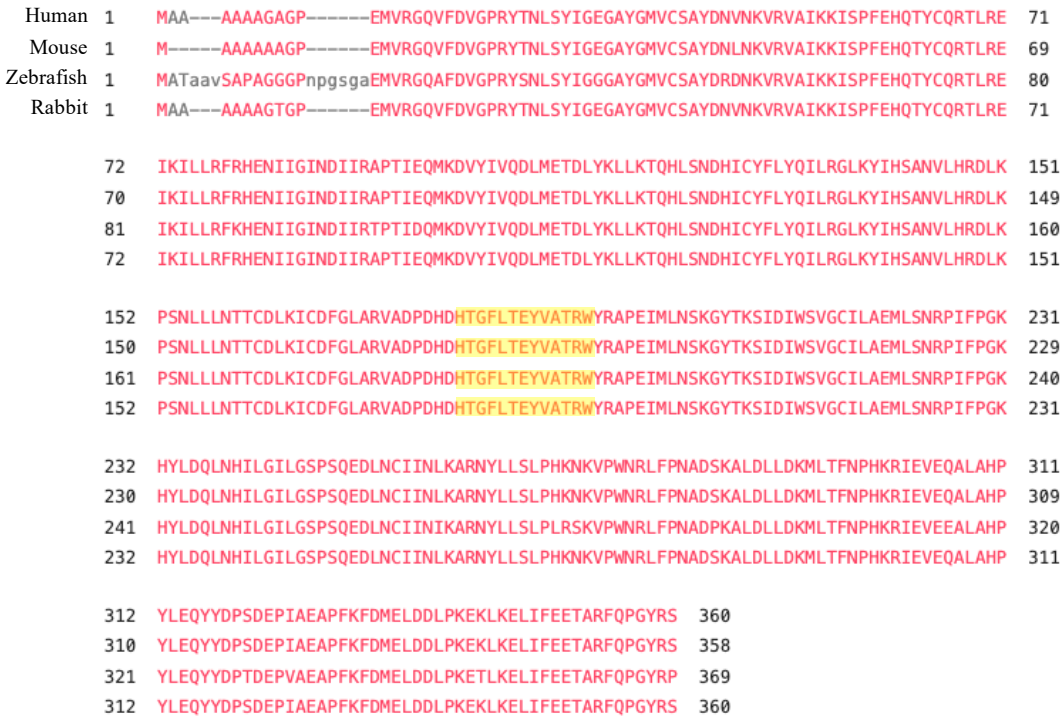

A.1 Gene sequence alignment of mitogen-activated protein kinase 1 (ERK1) for human, mouse, zebrafish, and rabbit. Sequences aligned using COBALT RID (Papadopoulos and Agarwala, 2007). Sequence highlighted in yellow represents the phosphopeptide sequence used to block mouse-anti-phosphoERK1/2 (Thr202, Tyr204) monoclonal antibody (Invitrogen, Cat# 14-9109-82) immunoreactivity (Chapter 2).